General Disclaimer

One or more of the Following Statements may affect this Document

- This document has been reproduced from the best copy furnished by the organizational source. It is being released in the interest of making available as much information as possible.

- This document may contain data, which exceeds the sheet parameters. It was furnished in this condition by the organizational source and is the best copy available.

- This document may contain tone-on-tone or color graphs, charts and/or pictures, which have been reproduced in black and white.

- This document is paginated as submitted by the original source.

- Portions of this document are not fully legible due to the historical nature of some of the material. However, it is the best reproduction available from the original submission.

NASA

Technical Memorandum 83971

THE MULTI-PARAMETER REMOTE MEASUREMENT OF RAINFALL

David Atlas, Carlton W. Ulbrich
and Robert Meneghini

JULY 1982

NASA TECHNICAL MEMORANDUM

THE MULTI-PARAMETER REMOTE MEASUREMENT OF RAINFALL

by

David Atlas[1], Carlton W. Ulbrich[2] and Robert Meneghini[1]

[1]Goddard Laboratory for Atmospheric Sciences (GLAS)
NASA/Goddard Space Flight Center
Greenbelt, Maryland

[2]Clemson University
Clemson, South Carolina

July 1982

NASA Goddard Space Flight Center

TABLE OF CONTENTS

Abstract

This paper is a critical survey of the measurement of rainfall by remote
sensors. One parameter radar rainfall measurement is limited because both
reflectivity and rain rate are dependent on at least two parameters of the
drop size distribution (DSD), i.e., representative raindrop size and number
concentration. This paper extends earlier work to develop a generalized
rain parameter diagram which includes a third distribution parameter, the
breadth of the DSD, to better specify rain rate and all possible remote
variables. Simulations show the improvement in accuracy attainable through
the use of combinations of two and three remote measurables.

The spectrum of remote measurables is then reviewed. These include path
integrated techniques of radiometry and of microwave and optical
attenuation. One carefully designed short path microwave attenuation
experiment is sufficiently persuasive to show that the disappointing
results achieved in many others was due largely to a combination of rain
sampling problems and vertical air motions between the path and the gages.
Also, when paths are colinear, attenuation deduced from radar and
radiometry are in good agreement with that measured directly. By and
large, dual wavelength radar methods which were aimed at improved
measurements in small range increments have proven disappointing. However,
when the attenuation estimated in this way, or by radiometry, is used as a
constraint on the retrieval of rain profiles from the radar, the results
are more promising. Selected experiments involving combinations of two or
more of the three measurables, radar reflectivity, attenuation, and/or

radiometry, show considerable promise when adequate account is taken of the sampling and air motion problems. The best results in gate-by-gate measurements have been achieved with dual polarization or differential reflectivity (Z_{DR}). However, even these have failed to meet their full potential because rainfall often does not behave according to apriori assumptions. An accompanying paper shows that the use of a third remote parameter in addition to Z and Z_{DR} offers great promise. In many cases, accuracy can be greatly enhanced and ambiguities resolved by personal examination of the radar displays which depict the nature of the bright band, cell spacing, homogeneity, and drop size sorting effects. With a growing appreciation of the needs and the capabilities of the various techniques, the future of highly improved remote rainfall measurements seems bright.

1. Introduction

The multi-parameter measurement of precipitation is the result of the relatively recent recognition of the facts pointed out many years ago that both the rainfall rate, R, and the radar reflectivity factor, Z, were functions of at least two parameters of the drop size distribution (DSD), namely representative drop size and number concentration. Indeed, both R and Z are also functions of the breadth of the DSD. As a result, it is not possible to utilize a single Z-R regression relationship for all types of rain; nor is it possible to account for space and time variations from the mean Z-R law which are due to fluctuations in the DSD induced by a variety of physical processes. This paper reviews the work done to measure rainfall more accurately without any apriori assumptions about the DSD through the use of additional remotely measurable parameters such as microwave and/or optical attenuation (Ulbrich and Atlas, 1978), differential reflectivity (Seliga and Bringi, 1976), and microwave radiometry.

We concentrate almost exclusively on rainfall and exclude snow and hail except as the characteristics of the former may be used indirectly to infer features of the rain. We allude to hail mainly when it may be confused with rain. We also note that this is a selective, not a comprehensive review. Thus, while we shall refer to the original work for basic concepts, we shall omit many others and cite only those which appear to have been pivotal in the development of a branch of thought.

2. Background

It is over 40 years since Ryde (1941, 1946) first showed the
relationships between the reflectivity and attenuation of microwaves and
rainfall rate and thus set the foundations for radar measurements of
precipitation, and indeed, for all of radar meteorology. It was Wexler and
Swingle (1947), Marshall et al. (1947), Atlas (1947, 1948), and then
Marshall and Palmer (1948) who turned Ryde's work, which was concerned with
precipitation as unwanted clutter, toward the meteorological applications
of radar. Following Marshall et al. (1947), Austin and Williams (1951)
were the first to conduct thorough quantitative experiments on the relation
between echo intensity and rain rate. Austin and Richardson (1952) then
noted that the relations depended on the rainfall type. This, and the
subsequent work by Blanchard (1953) in which he showed major differences
between orographic and non-orographic rains in Hawaii were among the first
signs that there was not a universal relationship between the reflectivity
factor, Z, and rain rate, R.

In spite of the persuasive evidence which had already been gathered by
the mid-50's (Twomey, 1953) that one could not hope to determine R from a
measurement of Z alone and a simple Z-R relation, much of the community
persisted in this vain hope. Of course, it was also hoped that one could
find Z-R relations appropriate to either the regional climate, to the
observable weather parameters, or to rainfall type. Attempts to devise
such classification schemes have been reported by Cataneo (1969) and by

Cataneo and Stout (1968). The result is that by 1970 Battan (1973) reported 69 Z-R relations from many places around the world. It is safe to say that that number has probably doubled in the last decade. Further attempts to resolve these problems have involved averaging in space and time the rainfall rates determined from Z-R relations to deduce storm totals. Wilson and Brandes (1979) review this work and conclude that considerable averaging is required to obtain radar measured rainfall which is within a factor of two of the true rainfall 75% of the time.

In recognition of the wide variation in Z-R relations, Atlas and Chmela (1957) proposed a physical basis for those relations and developed a rain parameter diagram (see also Atlas, 1964) involving the four basic parameters, Z, R, W (rain water content), and D_0 (the median volume drop diameter). Plots of the various observed Z-R laws on the diagram showed dramatically that the variations were due largely to differences in the association between D_0 and R and that the latter did not usually correspond to that found by Marshall and Palmer (1948) and Atlas (1953) for stratiform rainfall. In short, when rain is comprised of many small drops of low fallspeed, the liquid water content is bound to be higher and the reflectivity lower than with an equal rain rate of large fast falling drops. The result would be an erroneous value of R as deduced from a Z-R relation. Moreover, these variations can occur from day to day, place to place, and moment to moment, especially as a result of size sorting.

Among other things, Atlas and Chmela (1957) showed that rain rate, R, could be expressed as a function of Z, D_0, and G, where the latter quantity

is a dimensionless moment of the mass distribution which increases with the breadth of the distribution (Atlas, 1964). In other words, an accurate specification of R depends not only upon the measurement of Z but also upon the measurement of both D_o and G, or proxies thereof.

These facts should be recognized as well from the nature of any drop size distribution (DSD) such as that of Marshall-Palmer, viz.,

$$N = N_o \exp(-\Lambda D) \tag{1}$$

where N_o and Λ are parameters of the distribution with Λ expressible in terms of D_o through $\Lambda D_o = 3.67$ (Atlas, 1953). Marshall and Palmer (1948) take N_o to have a specific value independent of rainfall rate, viz., $N_o = 8 \times 10^4$ m^{-3} cm^{-1} and Λ to vary as $\Lambda = 41 R^{-0.21}$ or, alternatively, $D_o = 0.09 R^{0.21}$. Embodied in their result is the explicit assumption that one of the distribution parameters is constant so that the distribution is a function of only one variable parameter, viz., D_o. If this assumption were strictly true then all integral quantities defined in terms of N(D) would be dependent on only one parameter and would therefore all would be uniquely expressible in terms of any other integral parameter. That such is not the case is clear from the work of Waldvogel (1974) and Donnadieu (1980) who show that N_o and D_o can undergo sudden, independent, very large changes in rainstorms. Consequently, these integral quantities are functions of two independent parameters and possibly more if it is necessary to specify distribution parameters such as the breadth and the

upper and lower limits D_{max} and D_{min}, respectively.

Having recognized that the remote measurement of rainfall rate required at least two independent parameters, Ulbrich and Atlas (1978) generalized the diagram of Atlas and Chmela (1957) to include additional parameters as shown in Fig. 1a. This diagram contains the isopleths of Z, R, W, and D_o as in Atlas and Chmela (1957) but also carries isopleths of N_o and optical extinction Σ. On separate overlays isopleths are shown for total number concentration N_T and microwave attenuation A (λ) at radar wavelengths λ = 0.86, 1.25, 1.778, and 3.22 cm. The temperature dependence of A(λ) is also included. A typical attenuation overlay is shown in Fig. 1b for λ = 3.22 cm. Since Seliga and Bringi (1976) showed that Z_{DR}, the differential reflectivity factor at orthogonal polarizations, is a unique function of D_o for an M-P DSD, the isopleths of D_o in this rain parameter diagram may be replaced by isopleths of Z_{DR} using the inset in Fig. 1a.

The nomogram of Ulbrich and Atlas is a powerful tool. Most importantly, by entering the diagram with any two of the 8 parameters (or 9 if Z_{DR} is included), the other 6 (or 7) are uniquely determined without apriori assumptions other than the basic one that the distribution is exponential. (See below for a generalization to other distribution forms.)

The diagram also demonstrates that an assumption of an empirical relationship between any two rainfall parameters necessarily implies relationships between all other pairs of parameters on the diagram. This conclusion is substantiated by Ulbrich and Atlas (1975) who show that all

of the empirical relations which can be established between pairs of rainfall parameters involve scatter in the experimental data about these relations which is directly related and of about the same relative magnitude. For example, the percentage deviation of an experimental data point from an empirically derived Z-R relation will be of about the same magnitude and have the same sense as the deviations of this data point from the corresponding empirically derived D_o - R relation.

An illustration of the use of the diagram is shown in Fig. 1c where several empirical Z-R relations have been plotted on a simplified version of the rain parameter diagram. Also shown as a shaded region is that area within which lie all of the 69 Z-R relations listed by Battan (1973). As indicated by Ulbrich and Atlas (1978) this shaded region spans a range of N_o values of almost 3 orders of magnitude and, for given Z, a range of R values of more than one order of magnitude. In addition, these Z-R relations generally cross both the N_o and D_o isopleths indicating that both Z and R are dependent on two distribution parameters each of which varies independently between successive observations. Attempts to improve the accuracy of prediction of Z-R relations by adjusting the coefficients and exponents will therefore be largely unsuccessful. Deviations found from use of such equations are the result of the natural variability in both N_o and D_o and cannot be simultaneously accounted for in a Z-R relation, but can be allowed for in dual-measurement methods.

From the above, it is apparent that we need to measure at least one independent parameter in addition to Z to obtain more accurate measures of

rainfall and to do so without any apriori Z-R relation. In a series of papers, Ulbrich and Atlas (1975, 1977) and Ulbrich (1981), have simulated the increased accuracy attainable through the use of combinations of microwave attenuation, A, and Z, optical extinction, Σ, and Z, and in an accompanying article in this volume (Ulbrich and Atlas, 1982a), the combination of differential reflectivity Z_{DR} and Z. All of these will be reviewed in Section 4 where it will also be shown that for some dual-measurement methods the determination of two parameters of the DSD results in a residual variance and/or bias in the specification of rain rate. Thus, in order to attain the "ultimate" in accuracy, one should measure a third parameter which is a function of the shape or breadth of the DSD. The effects of allowing for deviations in DSD shape from exponential on the structure of the rain parameter diagram are covered in Section 3. In Section 4, it is shown that by introducing a third remote measurable in experimental simulations, it is possible to eliminate the aforementioned systematic bias due to DSD shape variations.

The simulations of multi-parameter measurements by Ulbrich and Atlas are all based upon the computation of the remote measurables from several hundred samples of DSD's. Thus they do not include the measurement errors and practical limitations of actual remote sensing systems. Consequently, the "ultimate" accuracy demonstrated by these simulations assumes that the measurement technique involves combinations of perfectly measured remote measurables and not those which would be derived from a very dense raingage network which presumably would provide the ultimate measure of ground

truth.[1] We cover these problems in summary fashion in Section 5.

Also included in Section 5 is a summary of the various remote methods of measuring rainfall which have been proposed or actually utilized in the field. Included in this section is a brief history of single measurement techniques involving radar reflectivity, microwave attenuation, or similar measurables. The results obtained thus far from dual-measurement methods are also reviewed, which includes dual-wavelength radar methods, dual-polarization (Z_{DR}) methods, and combinations of radar and radiometer measurements. Special attention is paid to the apparent success of methods which involve path-averages. Excluded from this summary are direct methods such as raingages or even vertically pointing Doppler rada. located within the rain region as a means of calibrating the remote sensors or bounding the errors in correction algorithms. The former have been discussed by Hitschfeld and Borden (1954) and by Wilson and Brandes (1979). However, we shall discuss several approaches by which we may be able to infer features of the rainfall which are not directly measurable in Section 6.

3. Generalization of Rain Parameter Diagram

In the next section it is shown that the assumption of a two parameter exponential size distribution in a dual-measurement method of determining

---

[1] The sampling errors associated with individual gages and the gate spacing relative to storm size raise serious questions as to what really constitutes "ultimate" ground truth.

rainfall rate is, in most cases, adequate to achieve at least a five-fold increase in accuracy over that which results from the use of an empirical relation. However, for some combinations of remote measurables further improvement is possible if allowance is made for deviations of the experimental size spectrum from the assumed exponential form. The implication is that to achieve the maximum accuracy of measurement requires knowledge of the shape of the size distribution. Ulbrich and Atlas (1982a) describe methods by which the shape of the distribution could be determined either apriori or by direct measurement. They also present evidence for varying size distribution shape in nature through analysis of empirical Z-R relations of other workers. Further support for such shape effects is contained in the work of Blanchard (1953), Best (1950), and Mueller (1965). The latter work is especially significant since it involves rain drop size spectra collected by a photographic method that does not require knowledge of the drop fallspeed to find the size distribution and, in addition, has a much larger sampling volume than other methods. This method is used to find average drop size distributions from several locations around the world which in every instance are better described by a mathematical form which is closer to a gamma or log normal distribution than to exponential.

To show the effects of varying distribution shape on the structure of the rain parameter diagram it may be assumed that the distribution is of the form

$$N(D) = N_o D^m \exp(-\Lambda D) \quad (0 \le D < \infty) \qquad (2)$$

where the exponent m may have any positive or negative value. Such a form means that the distribution is now described by three parameters (N_o, Λ and m) and that one of them must be known apriori in a dual-measurement method or that a third measurable would have to be introduced if all three parameters were to be determined simultaneously. It should be noted that for this size distribution the parameter Λ is related to D_o, the median volume diameter, by the excellent approximation $\alpha_m = (\Lambda D_o)_m = 3.67 + m$. The important moment G introduced by Bartnoff and Atlas (1951) is given by

$$ G = \frac{\int D^6 N(D)\,dD}{D_o^3 \int D^3 N(D)\,dD} = \frac{(6+m)(5+m)(4+m)}{(3.67+m)^3} \qquad (3) $$

which varies monotonically from 5.2 to 1.8 as m varies from -2 to 2, respectively. As indicated by Ulbrich and Atlas (1982a), negative values of m correspond to broad, concave upward distributions, such as those found in orographically induced rainfall in Hawaii, whereas positive m corresponds to a narrow, concave downward distribution such as those found by Mueller (1965) for a variety of rainfall types and by Jones (1956) for thunderstorm rain.

In terms of the size distribution N(D), the quantities plotted on the rain parameter diagram are defined by equations specified in detail in Ulbrich and Atlas (1978). The definitions of W, Z, Σ, and N_T all yield

results which can be expressed simply as a product of the three factors N_o, a power of D_o, and a function of m when Eq. (2) is used for the size distribution. The integrals defining R and A would be done numerically unless it is sufficiently accurate to adopt power law approximations of the form $v(D) = \gamma D^{0.67}$ ($\gamma = 17.67$m $s^{-1}cm^{-0.67}$) for the drop fallspeed in still air as in Atlas and Ulbrich (1977) and $Q_t(D) = CD^n$ for the microwave attenuation cross section as in Atlas and Ulbrich (1974). In the latter expression C and n would be dependent on radar wavelength and temperature.

From these definitions it can be shown easily that each of the quantities W, R, Σ, A, N_T and N_o can be expressed in terms Z, D_o and m through the general form

$$X = a_x \, \mu_x(D_o, \, m) \, ZD_o^{-e}x \qquad (4)$$

where the coefficient a_x, exponent e_x and function $\mu_x(D_o,m)$ are given in Table I with $\Gamma(a)$ equal to the complete gamma function, $\beta_m = \alpha_m^3/\Gamma(7+m)$ and $\alpha_m = (\Lambda D_o)_m = 3.67+m$. The functions $F_R(D_o,m)$ and $F_A(D_o,m)$ are defined in the table in terms of the numerical integrals involving $v(D)$ and $Q_t(D)$ in R and A, respectively. Also shown in brackets are the results for $\mu_R(m)$ and $\mu_A(m)$ when the aforementioned power law approximations for $v(D)$ and $Q_t(D)$ are used in $F_R(D_o,m)$ and $F_A(D_o,m)$. It is immediately apparent that the μ_x for W, Σ, N_T and N_o are all dependent solely on m so that for these quantities the effects of variation in size distribution shape (i.e.,

variations in m or G) are contained completely in the μ_x. The same remarks apply to the $\mu_R(m)$ and $\mu_A(m)$ in the case where the power law approximations are used. These μ_x can therefore be used to adapt the rain parameter diagram to distributions other than exponential (m = 0).

In making such an adaptation, the ordinate (or Z isopleths) and D_o isopleths are considered invariant and the labels on the remaining isopleths are multiplied by the ratio $\mu_x(m)/\mu_x(0)$ appropriate to the rainfall parameter and size distribution in question. These ratios for W, Σ, N_T and N_o are shown in Fig. 2 over the range $-2 \le m < 2$. Also shown is the variation of G with m and the ratio $\mu_R(m)/\mu_R(0)$ for the power law approximation to v(D). As an example of how to use these ratios, to construct a rain parameter diagram for m= 2, the Z and D_o lines are left unchanged and the W, Σ, N_T, N_o and R labels are multiplied by the ratios $\mu_x(2)/\mu_x(0)$ found from Fig. 2, viz., 0.76, 1.22, 0.49, 12.1, and 1.31, respectively. This example (m=2) is shown by Ulbrich and Atlas (1982a) to correspond to thunderstorm rain so that for this type of rain the W labels are reduced by 24%, the Σ labels are increased by 22%, the N_T labels are reduced by about 50% and the N_o labels are increased by more than an order of magnitude.

The ratios $\mu_A(m)/\mu_A(0)$ which would be used to relabel the microwave attenuation isopleths are almost identical to the $\mu_R(m)/\mu_R(0)$ in Fig. 2 in the case where the power law approximation to $Q_t(D)$ is used. In fact, for m > -2, λ < 3.22 cm and $-10 \le T \le 20^{\circ}C$ the $\mu_A(m)/\mu_A(0)$ are almost independent of λ and T, the maximum difference among these ratios being

only about 5%. For m = -2 the maximum difference is only 14%.

The accuracy of the use of the power law approximations to v(D) and $Q_t(D)$ for relabelling the isopleths on the rain parameter diagram has been determined by calculating the μ_R and μ_A using the numerically integrated results for $F_h(D_o,m)$ and $F_A(D_o,m)$ in Table I. The results so obtained are functions of both D_o and m and will be displayed in later work. It is sufficient here to note that the differences between the results obtained by numerical integration and those found using the power law approximations are only a few percent over the range $0.02 \leq D_o \leq 0.5$ cm for m > -2. For m = -2 the differences amount to about 10% over the same range of D_o's.

The remaining measurable on the rain parameter diagram, viz., Z_{DR}, can be adjusted for size distribution variations using the results of Ulbrich and Atlas (1982a). The latter work shows that this quantity can be approximated closely by the form

$$Z_{DR} = C_m D_o^{1.5} \tag{5}$$

where Z_{DR} is in db and D_o is in cm. Only the coefficient C_m is dependent on distribution shape and its variation with m is shown in Fig. 2. Since Z_{DR} is a function of D_o only for given m, these results can be used to transform the D_o scale on the rain parameter diagram to a Z_{DR} scale.

4. Simulations of Remote Rainfall Measurement

Raindrop size spectra have been used by many investigators to simulate

remote radar measurements so as to discover the relationships between these measurables and the rainfall parameter of interest. The earliest and best known of these simulations uses raindrop size spectra to calculate the radar reflectivity factor Z and the rainfall rate R from which data a relationship of the form $Z = aR^b$ is found by standard regression methods. The accuracy of prediction of such an empirically determined relation can then be tested by finding Z from the drop size spectrum, calculating R from Z in the empirical Z-R relation, and comparing the result so obtained with R found from the drop spectrum. Such a simulation involves a comparison of rainfall rates determined using a simulated remote single-measurement Z-R technique with those found from a simulated raingage measurement. Of course, it does not include complications due to effects such as vertical and horizontal winds, differences in size and location of the measurement volumes of the radar and raingage, instrument errors in either the radar or raingage, and other effects. In other words, the comparison is between two presumably perfectly measured quantities and the accuracy of prediction which results from such a simulation is the best that could be expected in nature with the use of a single-measurement technique.

Examples of such approaches to rainfall rate measurement simulation are far too numerous to review here. It is sufficient to show as illustrations of the kinds of results obtained from such analyses those given by Ulbrich and Atlas (1977), Atlas and Ulbrich (1977), and by Ulbrich (1981). Each of these investigations uses raindrop size spectra collected with a momentum disdrometer which were analyzed to determine empirical

relations between R and each of the remote measurables Z, Σ, and A. For the latter measurable several radar wavelengths were considered and the results are discussed in Atlas and Ulbrich (1977) and reviewed in the next section; in this section only those results for the wavelength $\lambda = 3.22$ cm are illustrated. The Z-R, Σ-R and A-R relations found from these empirical analyses were then tested for accuracy of prediction in the manner described above.

The results of the comparisons of the rainfall rates calculated from the empirical relations (R_{calc}) with those found from the size spectra (R_{actual}) is shown in Fig. 3. The upper, middle and lower sets of data points correspond to R_{calc} found from the empirical Z-R, Σ-R, and A-R relations, respectively. It is clear that the accuracies of prediction of these three single-measurable empirical relations are comparable. The average absolute deviation (AAD) (i.e., the average deviation without regard for sign) of R_{calc} from R_{actual} is 33% for the Z-R relation, 37% for the Σ-R relation, and 24% for the A-R relation. Similar results are obtained for other remote measurables and rainfall parameters, i.e., the accuracy of prediction of empirical relations between any of Z, Σ or A and any rainfall parameter, such as R, W, D_o, etc. is similar. Only in the special case of $\lambda \sim 1$ cm does the empirical A-R relation produce significantly better agreement between calculated and actual rainfall rates. The fortuitous circumstances which produce this good agreement are described by Atlas and Ulbrich (1977) and reviewed in the next section.

The origins of the limitations on the accuracy of prediction of these

empirical relations have been discussed earlier in Section 2 where it was concluded that it requires at least two remote measurables to determine rainfall parameters accurately. Support for the latter conclusion has been presented by Ulbrich and Atlas (1975, 1977, 1982a) and Ulbrich (1981) who use drop size spectra to simulate dual-measurement techniques. The pairs of measurables which have been considered in these investigations are (Z, A), (Z, Σ) and (Z, Z_{DR}). The first of these pairs consists of those measurables determined by a dual-wavelength radar with one attenuating wavelength and a second for which the Rayleigh approximation is valid. Alternatively, a radiometer may be used to estimate A albeit a path-averaged value (see Section 5). The second corresponds to a system employing a radar and a lidar, laser or optical transmissometer. The third pair represents those measurables acquired by a dual-polarization radar. In simulations of these dual-measurement methods, the size distribution is assumed to depend on two parameters (such as N_o and D_o in Eq. (2) with m given) so that each of the remote measurables and the rainfall rate are all functions of these two parameters. The experimental size spectra are used to compute values of the two measurables in question which are then combined by simple elimination between the two relevant defining equations (see Ulbrich and Atlas, 1978) to find the two distribution parameters. These distribution parameters are then used to find a calculated value of rainfall rate (R_{calc}) as deduced from the pair of measurables. The result so obtained can then be compared with the actual rainfall rate (R_{actual}) as found from the drop size spectrum in the same fashion as for the empirical

analyses described above.

Comparisons of rainfall rates formed by such dual measurement simulations with the actual values are shown in Fig. 4. The upper set of data points corresponds to a (Z,A) simulation described by Ulbrich (1981) with the attenuating wavelength $\lambda = 1.25$ cm. The AAD of the R_{calc} from the R_{actual} is only 5% for this set of data. The second set of data points also corresponds to a (Z,A) method but with $\lambda = 3.22$ cm and the AAD for this case is also 5%, indicating that the accuracy of this dual-measurement method is not dependent on the choice of the attenuating wavelength. Comparison of the accuracy of this method with that obtained above with the use of Z or A alone in an empirical relation shows that the improvement in accuracy is a factor 7 or 5 relative to the Z-R or A-R empirical methods, respectively.

The third set of data points in Fig. 4 represents a comparison of R_{calc} with R_{actual} for a dual-measurement method employing Z and Σ. Here the AAD = 8% so that the improvements in accuracy are factors of 4 and 3 relative to the Z-R and Σ-R methods. A closer inspection of this set of data points shows that there is a systematic offset of the R_{calc} below the R_{actual}. Ulbrich and Atlas (1977) show that this offset is due to deviations of the experimental size distribution from the assumed exponential form (i.e., Eq. (2) with $m = 0$). If a gamma distribution is used with $m = 2$ then the average offset of these data is reduced to zero and the AAD becomes less than 5%, indicating that the improvement in accuracy relative to empirical methods is at least as good as the (Z,A)

technique when the correct form of the size distribution is used. The
reason that the dual-measurement (Z, Σ) method is more sensitive to size
distribution variations than the (Z, A) method is that those distribution-
dependent factors involving Σ in the solution for R_{calc} are more strongly
affected by such variations than those which involve A. This can be shown
easily from the equations defining R, Z, A, and Σ in Table 1.

The last set of data points in Fig. 4 corresponds to a simulated
measurement technique involving Z and Z_{DR} where the former quantity in this
case refers to the reflectivity factor for horizontal polarization. This
simulation is the same as that described by Ulbrich and Atlas (1982) in
another paper in this volume who find the AAD = 27% when it is assumed that
m = 0 (i.e., an exponential distribution). However, when it is assumed
that m = 2 the comparison of R_{calc} with R_{actual} is as shown in Fig. 4 and,
as indicated by Ulbrich and Atlas (1982a), for this case the AAD = 13%,
indicating that this dual-measurement method is even more sensitive to size
distribution variations than those discussed above. That this is the case
is demonstrated by Ulbrich and Atlas (1982a) using an approach similar to
that described for the (Z, Σ) measurement technique using the defining
equations in Table I.

It may be concluded from these simulations that combinations of remote
measurables involving Z and A, such as those used in dual-wavelength radar
techniques, have potential for producing accurate estimates of rainfall
rate without the requirement of apriori knowledge of the size distribution
shape. In other words, for these methods only two remote measurables are

needed and it is sufficient to assume that the size distribution is exponential. For other techniques such as (Z, Σ) and (Z, Z_{DR}) variations of the distribution from exponential can produce significant effects which should be accounted for if these techniques are to realize their fullest potential.

Ulbrich and Atlas (1982a) describe methods by which the shape of the distribution can be determined; one of these involves the introduction of a third remote measurable. By so doing each of the parameters N_o, D_o, and m can be determined simultaneously for each data point, thereby allowing for changes in size distribution shape from moment to moment in the rainfall. One such method might use Z, Z_{DR}, and Σ as the triad of remote measurables and the results of a simulation for this case are shown in Fig. 5. From these data it is obvious that by accounting for changes in distribution shape it is possible to achieve very high potential measurement accuracy.

Of course, a system involving three simultaneously determined remote measurables poses profound problems for implementation. A simpler approach would be to estimate distribution shape in rainshafts using path-averaged measurements as described by Ulbrich and Atlas (1982a) and in a later section of this work. Alternatively, use may be made of the empirical observation that there is a close relationship between the parameters N_o and m within a given rain and between rainfall types which may be written approximately as $N_o = 0.2 \exp(3.5 \alpha_m)$ where $\alpha_m = (\Lambda D_o)_m = 3.67 + m$. This simple relationship, which is obeyed very well both within a given rainstorm and between different rainfall types, may be sufficient to allow

for changes in distribution shape without the need for the introduction of a third remote measurable.

The results of these simulations of multi-parameter methods indicate that these methods have high potential for determining rainfall rates accurately. However, we emphasize that these simulations embody the same assumptions as those for single-measurement simulations involving empirical relations. That is, it is assumed here that each of the measurables in the multiple-parameter scheme is measured perfectly, i.e., without instrumental error, and that the effects of complications such as vertical winds, turbulence, etc.., are minimal. As in the case of single-measurement simulations, the results presented here represent the ultimate accuracy attainable by methods employing more than one remote measurable. In spite of these simplifying assumptions these simulations reveal the origins of the failure of empirical methods and demonstrate the potential improvement which is possible.

5. Remote Measurement Methods

This section deals with the various remote measurement methods which exploit radar, microwave links, and/or radiometry either singly or in combination. In the case of radar we assume that the reader is familiar with or has access to the literature for the accurate measurement of echo power and the determination of the reflectivity factor for single wavelength relations to rainfall (Atlas, 1964; Battan, 1973). Dual wavelength radar methods generally involve the measurement of echo power at

two or more range gates at two wavelengths aimed at the measurement of rainfall attenuation. Dual polarization radar or the so called differential reflectivity technique provides yet another approach to obtain a parameter which is sensitive to a representative drop size.

Rainfall can also be deduced from attenuation measured by either a radar or a continuous wave transmitter viewing one or more retroflectors through the rain, or simply transmitting on a one way path to a receiver. Such one way paths may be from ground to ground, to aircraft, or to space. Also, microwave radiometers viewing the sun or the absorbing medium itself provide excellent proxy measurements of attenuation, and when combined with radar or other means of deducing the rain path-length, give average rain rates. And of course, we have also alluded to the utility of optical extinction in previous sections.

All of these methods and combinations thereof will be discussed in this section along with examples of experiments which demonstrate their utility and limitations. Because of their simplicity and the abundance of the literature on the subject, we begin with a brief discussion of radiometric techniques followed by methods of measuring path integrated attenuation or deducing it from either or both microwave radiometers and radar.

5.1 Radiometry

For meteorological applications, radiometry was originally introduced as a proxy for the path integrated attenuation. Since it comes into the

present work in a variety of contexts, we shall discuss it briefly here.
The following treatment follows that of Hogg and Chu (1975). Radiometers
tracking the sun or simply viewing the rain filled sky were introduced
largely by the space communications community to obtain proxy data for
attenuation. We shall not treat the suntracker because it is too
restricted in its pointing requirements, although it has a considerably
wider dynamic range than passive radiometers in measuring attenuation and
provides an excellent calibration for the latter.

The brightness temperature, T_b, measured by a passive microwave
radiometer may be expressed as

$$T_b = T_a \left[1 - \exp\left(-\sigma x\right) \right] \qquad (6)$$

where T_a is the apparent temperature of the absorbing rain medium and σ its
attenuation coefficient in cm^{-1}; x is distance in cm. Recall that

$$\sigma(cm^{-1}) = 2.3 \times 10^{-6} \, A \, (db \, km^{-1}) \qquad (7)$$

Thus the total attenuation is

$$AL = -10 \, Log \left(1 - T_b/T_a\right) \qquad (8)$$

where L is the total path length in km.

Hogg and Chu discuss various methods of obtaining the apparent medium temperature T_a. Probably the best approaches are to use either a suntracking radiometer or a space earth communications link. These provide measures of true attenuation (i.e., AL) which, with measured values of T_b, permit estimates of T_a. Despite the fact that the temperature of the rain varies with height and season, measurements ranging from North Carolina to Ottawa gives values of T_a between 270 and 273 K (Strickland, 1974; Ippolito, 1971). This is due to the scattering of the cold sky by the drops, an effect which increases with both rain rate and radio frequency (Zavody, 1974). Hogg and Chu conclude, that for statistical purposes, one may use $T_a = 273K$ for conversion of T_b to attenuation at frequencies of the order of 20 GHz over much of North America. For individual measurements of path attenuation, one needs to use more accurate approximations to T_a.

Measurements of attenuation deduced from a 16 GHz radiometer are compared to simultaneous 15.3 GHz attenuation values as measured with the ATS-5 satellite in Fig. 8 (Penzias, 1970). The accuracy is excellent although the maximum is only 5 db. Similar measurements by Strickland (1974) discussed below show somewhat greater variance.

It is clear from Eq. (8) that as the rain attenuation increases T_b approaches T_a exponentially. Thus when exp $(-cx) = 0.1$ (and AL = -10db) $T_b/T_a = 0.9$; i.e., the T_b/T_a curve is near saturation. While measurements of T_b can generally be made to accuracies of about 0.1 to $1^{O}K$, the possible variations in specifying T_a are such that there is general agreement that passive microwave measurements should not be used for attenuations larger

than 10 db. To obtain a sufficiently large dynamic range in radiometric measurements of rainfall will require two or more wavelengths. Each doubling of the specific attenuation coefficient attained by increasing the wavelength will result in a twofold increase in the maximum $\bar{R}L$ product where $\bar{R}$ is average rain rate and L is the total path through rain. Fig. 9 (after Lu (1978) presents curves of T_b versus $\bar{R}$ for a 3.2 cm radiometer for various path lengths, L. The calculations include the effects of oxygen and water vapor. Note that the curves all saturate at $\bar{R}L$ product of about 1000 (mm h^{-1} km) and that the useful dynamic range is just about two decades in rain rate. Of course, the shorter wavelengths saturate at smaller $\bar{R}L$ values and have correspondingly smaller dynamic ranges. In nine comparisons to average rain measured by a surface network Lu (1978) found that the radiometer underestimated the observed rain by a mean of only about 8%. The rain path length was determined by radar.

It is useful to note that at wavelengths at which the attenuation coefficient is close to a linear function of rain rate, we have found (not shown here) that the measured T_b is essentially independent of the distribution of R along the path.

5.2   Path Integrated Attenuation

5.2.1 Ground to Ground

Because it was recognized long ago (Gunn and East, 1954) that the attenuation of microwaves of about 1 cm wavelength was essentially linear with rain rate, Collis (1961) and Godard (1965) attempted to measure

rainfall from the 0.86 cm attenuation of echoes between two fixed targets spaced some distance apart. The idea is that the measurement is then independent of the absolute calibration. Harrold (1967) following the lead of Collis and Godard did the most careful study of this approach using an 0.86 cm radar, two corner reflectors 6.9 km apart, and 8 rain gages along the intervening path. He found a mean attenuation coefficient of 0.27 R db/km in excellent accord with theory. Ratios of attenuation deduced cumulative rainfall to gage values fell within $\pm$ 20% in all but 6 of 23 cases.

The radio science literature is replete with measurements of attenuation along one way paths from transmitter to receiver at a broad range of wavelengths. In an early study comparing theory and measurement Medhurst (1965) reported disappointing results. He found very wide scatter and a clear tendency for measured attenuations to exceed maximum theoretical values (i.e., those corresponding to monodisperse drop sizes having the maximum extinction cross-section). In view of the findings of Atlas and Ulbrich (1977) showing excellent correlations between attenuation and rain rate computed from drop size spectra, and their conclusion that the attenuation near 0.9 cm wavelength was very insensitive to the drop size distribution, it is at first surprising that the path measurements should show such wide scatter. It is also curious that Harrold (1967) and his predecessors failed to get better rainfall measurements using the 0.86 cm radar target attenuation method. The only 35 GHz path-average measurements which agree well with theory are those of Norbury and White

(1972) which were made over a very short two way path of only 448 m (224 m doubled) and used four fast response rain gages along the path giving an average spacing of only 56 m between gages. Perhaps more important in the context of our subsequent discussion of sampling errors and the effects of up- and downdrafts is the fact that 3 of the 4 gages were on 3 m high poles, just 2 m below the microwave path, and they were sampled at 10 sec intervals. It is also pertinent to note that the polarization was vertical. Their results given in Fig. 6, show remarkably small scatter and agree reasonably well with theory. They found $A = 0.24 R$ compared to $A = 0.20 R$ db km^{-1} for vertical polarization reported by Atlas and Ulbrich (1977). On the other hand, the data of Semplak and Turrin (1969) at 18.5 GHz (Fig. 7) show much greater scatter and are more typical of the results reported in Medhurst's (1965) review.

Hogg and Chu (1975) provide the following reasonable explanations for the observed discrepancies and scatter.

Rainfall is apparently overestimateu from attenuation when:

   o Rain cells or maxima pass between gages.

   o Gages have slow response or are sampled infrequently.

   o Gages do not catch all rain; the error increases with windspeed.

   o An updraft occurs within the microwave path thus reducing the mean
       drop fallspeed and enhancing the liquid water content and
       attenuation in the path.

   o Oblate drops attenuate horizontal polarization more than vertical;

this was not recognized in early experiments.

o Failure to account for wetting of antenna radomes.

Rainfall is underestimated when:

o Downdrafts in the path increase mean drop fall speed.

o Polarization is vertical.

It is noteworthy that Semplak and Turrin (1969) had clear evidence of strong convergence and an updraft on October 25, 1967, when they measured consistently larger than theoretical attenuations at 18.5 GHz. The data for this case are shown by the crosses in Fig. 7. An updraft of only 1 m s^{-1} would explain this apparent discrepancy. Joss et al. (1974), using a vertically pointing Doppler radar, also found updrafts when measured attenuation aloft exceeded that calculated from DSD at the ground. This also explains the factor of 2 excess attenuation (in decibels) found by Anderson et al. (1947) in a well designed experiment at 24 GHz on a 1.95 km path in orographic rain along the windward slope of Hawaii near Hilo. We also note that recent studies of so-called storm "downbursts" by Fujita (1981) provide persuasive evidence that strong downdrafts can occur in storms at only a few tens of meters above the ground. Similarly, with intense localized convergence, we will find strong updrafts.

The effects of up- and downdrafts noted above and of turbulence in general raises serious questions about the meaning of surface rain gage measurements. The rate at which the rain mass reaches the surface locally may be either enhanced by downdrafts or reduced by updrafts. Point to

point agreement between either attenuation or radar reflectivity above the ground and surface gage rainfall is therefore not to be expected except in very steady stratiform rain. (See the discussion of the work of Joss et al., 1974, in Section 5). However, over some scale approaching the size of the storm cell itself, one should expect these effects to average out. This suggests that excessive rainfall along one attenuation path should be balanced by a deficit elsewhere.

Several important implications arise from this discussion: (1) Provided one accounts for the non-meteorological errors listed above, including sampling, there is no reason to doubt that microwave attenuation is indeed an excellent measure of the rain mass, and in the absence of vertical air motions, of rain rate. (2) However, if one is to use attenuation as a measure of local rain rate, which is only physically meaningful near the ground in any case, one must also measure the difference in vertical air motion between the heights of the attenuation path and the gages. (3) One must exert caution in utilizing surface rain gage statistics to infer fade statistics especially in convective storms; attenuation data derived from radiometers or radars elevated along the path of the microwave link should generally be satisfactory with the provisos noted below.

In short, we are convinced that once one accounts for the various error sources noted above, utilizes both vertical and horizontal polarization, and measures vertical air motions in the path, we should find the excellent relations between attenuation and path averaged rain rate

simulated by Atlas and Ulbrich (1978), and demonstrated experimentally by Norbury and White (1972). Indeed, it would appear that a folded 0.86 cm microwave path such as that of Norbury and White or one which traverses a square of perhaps 100 m on a side and is elevated only 5 to 10 m above the ground would provide a quantum improvement on any rain gage system covering a comparable area.

5.2.2 Ground to Ground; Optical Extinction

The use of electromagnetic radiation in the optical wavelength band for the measurement of rainfall has not been used to any great extent because of the obvious imitations of the method due to the presence with rain of fog and/or cloud droplets. The latter are usually abundant in widespread stratiform rain and severely attenuate a light beam. However, in heavy isolated showers their effects are not so pronounced and a limited number of experiments have been performed in these conditions using coherent optical radiation.

Atlas (1953) was the first to relate optical extinction to rainfall rate. Using the Marshall and Palmer (1948) drop size distribution he found a theoretical Σ-R relation of the form $\Sigma = 0.31 \, R^{0.67}$ whereas his empirical analysis of raindrop size spectra yields $\Sigma = 0.20 \, R^{0.68}$. The latter results agree fairly well with the empirical analysis of Ulbrich and Atlas (1977) who find $\Sigma = 0.18 \, R^{0.69}$.

Wilson and Penzias (1966) measured attenuation of a 10.6 µm maser beam

by showers along a 2.6 km path in New Jersey and found maximum extinctions of 12 db km^{-1} in rainfall rates of about 50 mm h^{-1}. This agrees very well with the theoretical prediction of Atlas (1953).

A carefully performed experiment using laser radiation has been reported by Chu and Hogg (1968) in heavy showers. Their theoretical relation for $\lambda = 0.63$ μm was calculated using the Laws and Parsons (1943) size spectra and can be represented very well by the form $\Sigma = 0.23 \ R^{0.69}$. This result agrees well with Atlas (1953) after correcting for the difference between the Marshall and Palmer (1948) and Laws and Parsons (1943) spectra. Chu and Hogg (1968) also present theoretical results which include corrections for beam broadening and forward scatter and which can be represented by the form $\Sigma = 0.16 \ R^{0.69}$. Most of the experimental measurements of Chu and Hogg (1968) are in better agreement with the empirical relation of Atlas (1953) given above than with the latter theoretical result.

The most successful use of coherent optical radiation to measure path-average rainfall rate has been reported by Wang et al. (1979). They use a system which detects the Airy diffraction-interference pattern produced by a raindrop falling through a collimated laser beam with path length of 140 m and diameter of 20 cm. Since the system produces a signal for every raindrop which falls through the beam that is directly related to the size of the drop, the method is not subject to errors induced by the assumption of a specific form of the size distribution. In fact, the path average size distribution of the drops can be determined from the data.

Wang et al.(1979) display results for N(D) for steady rain which are in very good agreement with the Marshall and Palmer (1948) distribution. The results found from these distributions for the rainfall rate R are compared with those deduced from a tipping bucket raingage immediately below the laser beam and are shown to be in very good agreement. The system has several advantages over other remote measurement systems, the major one being that prior knowledge of the size distribution is not required. However, its usefulness is restricted to situations where fog and cloud do not seriously affect the measurements.

5.2.3 Earth to Space

In recent years there have been a great many studies of path integrated attenuation and its relation to rainfall by the space communications community. Much of the relevant literature is summarized in a fine NASA handbook by Kaul et al. (1980), and in a series of comprehensive review papers by Oguchi (1981), Fedi (1981), Brussaard (1981), Olsen (1981), and Cox (1981). The previously cited paper by Hogg and Chu (1975) is also most valuable. An extensive series of papers reporting on propagation through precipitation is also found in a European Space Agency report on ATS-6 propagation Experiments in Europe (European Space Agency, 1977). From our point of view, the most interesting of the above papers are those which compare attenuation to rainfall as measured by rain gages under the path, to attenuation and or rainfall as deduced by radar, and to attenuation as inferred from microwave radiometry. Space

permits discussion of only a few of the key references.

5.2.4 Multi-Parameter Measurements in Space Communications

The importance of reliable microwave earth-space links at frequencies
in excess of 10 GHz has led to the need for path statistics on attenuation
and rainfall. This in turn has led to the widespread use of radiometers
and radars to deduce path attenuation. Strickland (1974) used 15.3 GHz
radiometer deduced attenuations for direct comparison to 15.3 GHz
attenuation on a link to ATS-5. Typical results are shown in Fig. 10.
Standard deviations of the differences range from 0.25 db at 3 db loss to
1.2 db at 8 db loss. The 1:1 line corresponds to an assumed effective
medium temperature of 278K; the bounding curves to a variation of $\pm$ 10K.
All the data fall nicely within these bounds. Strickland also used a 3 GHz
colocated radar directly along the same path and computed the 15.3 GHz
attenuation through the combination of the radar relationship $Z = 200 \ R^{1.6}$
and the appropriate A-R relation. After adjustment of the radar constant,
agreement with measured attenuations was said to be "generally good for
most meteorological conditions."

A well designed radar/attenuation experiment was also executed by
McCormick (1972). He measured path attenuation between three transmitters
mounted on an aircraft flying along a circle of constant radius from the
receiver site. A colocated 2.9 GHz radar was used to measure reflectivity
versus azimuth at the elevation angle corresponding to the attenuation
path, and to compute the attenuation based upon a method similar to that of

Strickland (1974). Fig. 11a shows a combined display of the radar PPI contoured in reflectivity according to the inset legend, and an azimuthal plot of 15.3 GHz attenuation in decibels along the periphery for September 24, 1968 at times shown along the outer scale. Fig. 11b presents comparisons of the measured attenuations at 4, 8, and 15 GHz (heavy lines) to those calculated from the radar data (thin lines). McCormick found that the radar data could be used to predict attenuation well provided the hydrometeors are liquid. However, gross overestimates of attenuation occurred when either hail or a bright band occurred.

Goldhirsh (1976) improved upon the aforementioned studies by using a well calibrated high resolution radar and a network of rain gages and disdrometers under the earth-space path which comprised 13 and 18 GHz transmitters on an uplink to receivers on board ATS-6. When a bright band was present on the radar, the attenuation integral based upon the radar data was terminated just below the band. In convective storms without a bright band, the integrals were carried along the earth-space path to zero echo. Correlations were generally excellent as shown in Fig. 12. Goldhirsh also computed Z-R and A-R relations based upon drop size spectra measured at the transmitter site, and also upon DSD's from Marshall and Palmer (1948)and Joss et al. (1968). For 18 GHz, calculated attenuations differed from measured values by only 1.3 db rms using his own DSD's, and by 1.6 and 2.1 db for M-P and Joss et al., respectively.

We conclude from the multi-parameter path integrated studies that the radar reflectivities and attenuation, either as measured by earth-space (or

earth-aircraft) microwave links, or as deduced from passive radiometers are highly consistent with one-another when the scatterers/absorbers are radar detectable liquid drops. Indeed, the correlations are remarkably good and are free of the tremendous scatter found in either attenuation-rain gage or reflectivity-rain gage data. This is clearly due to the fact that in the path comparisons (i.e., radar, microwave link, radiometer) the measurements are colocated and not subject to all the errors previously discussed in using spaced surface gages to represent the rain mass along a continuous path some distance above.

It is useful to note that McCormick (1972) actually used the difference between the radar calculated and the measured attenuation as a means of calibrating the radar. Since the difficulties of using rain gages and disdrometers to calibrate radar are not unlike the aforementioned problems associated with their use along microwave paths, the latter method commends itself for purposes of radar calibration.

5.3 Some Multi-Parameter Experiments in Radar Meteorology

Until recently few institutions working in radar meteorology have had either the resources or the motivation to conduct multi-parameter experiments corresponding to those in space communications.

It was largely as a result of the impetus provided by the differential reflectivity (ZDR) technique (Seliga and Bringi, 1976) that serious interest in the enhanced measurement of rainfall by the combination of parameters was revived. It is therefore not surprising that actual

experiments of this kind were sparse until the last few years.

5.3.1 Dual Wavelength Methods

One of the first discussions of the use of a combination of
reflectivity factor at one wavelength with relative attenuation at another
wavelength to deduce raindrop sizes was presented by Austin (1947). Atlas
(1954) suggested a similar method which would use dual-wavelength radar to
measure cloud liquid water content. Several of the assumptions made have
been carried over into much of the subsequent work: (a) for a range gate
containing liquid hydrometeors, the reflectivity factor is nearly
independent of wavelength, (b) the appropriate measure for a
dual-wavelength radar is over a path interval rather than a single range
bin, (c) the attenuation can be related to the liquid water content (or
rain rate) by means of an empirical relationship.

One of the primary interests of this method has been its potential for
hail detection (Eccles, 1975; Carbone, 1972). Although earlier work (Atlas
and Ludlum, 1961) had considered the logarithm of the ratio of return
powers from S-band and X-band radar, Eccles and Atlas (1973) showed that
the derivative of this quantity with respect to range is a more reliable
indicator of the leading and trailing edges of a hail shaft. However,
Srivastava and Jameson (1977) showed that there are serious problems of
interpretation of the hail signal for certain combinations of hail size
distribution parameters. An important consequence of the technique of
Eccles and Atlas (1973) is that in the absence of hail, the interval

attenution can be estimated. More detailed descriptions and error analyses of the method have been given by Kostarev and Chernikov (1968), Sulakvelidze and Dadali (1968), Eccles and Mueller (1971), and Eccles (1979).

For rain rate determination, the essentials of the method can be deduced from the radar equation and a ratio of powers. The return power P from a range r_j at wavelength λ_i is approximated by

$$P(\lambda_i, r_j) = \frac{C_i\, Z(\lambda_i, r_j)}{r_j^2} \exp\left[-0.46 \int_0^{r_j} A_i(x)\, dx\right] \tag{9}$$

where C_i is the calibration constant, Z, in mm^6/m^3, is the reflectivity factor and A_i in db km^{-1}, is the attenuation coefficient at λ_i. For a dual wavelength radar with $\lambda_1 < \lambda_2$ and at two ranges r_j, r_k with $r_j > r_k$ a power ratio Γ_p can be measured, where

$$\Gamma_p = \frac{P(\lambda_1, r_j)\, P(\lambda_2, r_k)}{P(\lambda_1, r_k)\, P(\lambda_2, r_j)} \tag{10}$$

which, from the radar equation, can be expressed as

$$\Gamma_p = \frac{Z(\lambda_1, r_j)\, Z(\lambda_2, r_k)}{Z(\lambda_1, r_k)\, Z(\lambda_2, r_j)} \exp\left[-0.46 \int_{r_k}^{r_j} (A_1(x) - A_2(x))\, dx\right] \tag{11}$$

Assuming that

$$Z(\lambda_1, r_i) = Z(\lambda_2, r_i) \quad for \quad i = j \ or \ i = k \tag{12}$$

then

$$(r_j - r_k)(\bar{A}_1 - \bar{A}_2) \equiv \int_{r_k}^{r_j} (A_1(x) - A_2(x))\, dx = -5 \log \Gamma_p \qquad (13)$$

The interval averaged rain rate $\bar{R}$ or liquid water content $\bar{W}$ then can be estimated by means of empirical laws relating $\bar{A}$ to rain rate and liquid water content. In most applications the longer wavelength, λ_2, is chosen to be non-attenuating.

As compared with the standard Z-R method, this type of dual wavelength algorithm represents an improvement in that the estimate of R is independent of the radar calibration constant. Furthermore, the estimate is generally less sensitive to fluctuations in the drop size distribution (DSD), a reflection of the relative insensitivity in the A-R law to variations in the DSD (Atlas and Ulbrich, 1977). Nevertheless, there are limitations of the method. Perhaps the most severe problem is one of dynamic range. For an S-band/X-band combination, and at low rain rates, the method must be applied over fairly long path intervals to attain sufficient sensitivity. For an S-band/K-band pair, the major difficulty is saturation at the shorter wavelength whenever long path lengths or intense rain rates are encountered.

A second difficulty is the large numbers of independent samples that are required to reduce the variance in the power ratio measurement (Eccles and Mueller, 1971; Srivastava and Carbone, 1971). The errors can be decreased, however, by interval averaging (Eccles and Mueller, 1971).

Eccles (1979) has also described a fairly complex procedure, which uses averaging in both range and azimuth, and which chooses certain minimum points in Z $(\lambda_2, r)/Z (\lambda_1, r)$ through which a smooth curve is fitted. One other possibility is to employ a broad band transmitted pulse (Krehbiel and Brook, 1979) to increase the effective number of independent samples. This strategy, however, has the disadvantage of increasing the receiver noise and further restricting the dynamic range. A less severe error source arises from the assumption that the reflectivity factor is independent of wavelength: the bias that is introduced, however, will become larger as the separation between the wavelengths increases or as the interval rain rate becomes more variable.

Despite these problems, the results reported by Berjulev and Kostarev (1974) and Eccles (1979) show that this method can achieve more accurate rain rate determination than the standard Z-R method if carefully chosen averaging schemes are used.

In the Eccles and Mueller (1971) and Kostarev and Chernikov (1968) approach, R is computed from A through an A-R law. In addition, however, there is the possibility of first estimating a kind of mean two parameter DSD from their equations. This is outlined in the following development. Using the foregoing results and the definition of the attenuation coefficient, then for an attenuating wavelength, λ_1 and non-attenuating wavelength, λ_2, pair

$$5 \log \Gamma_p = -\int_{r_k}^{r_j} A_1(x)\,dx = -0.434 \int_{r_k}^{r_j}\int_D Q_t(\lambda_1, D)\,N(D,x)\,dD\,dx \qquad (14)$$

Moreover, if the radar equation is integrated between r_k and r_j and the definition of Z is used then

$$\frac{1}{C_2} \int_{r_k}^{r_j} P(\lambda_2, x) x^2 dx = \int_{r_k}^{r_j} Z(\lambda_2, x) dx = H \int_{r_k}^{r_j} \int_D \sigma(\lambda_2, D) N(D, x) dD dx \quad (15)$$

where $H = \dfrac{10^6 \lambda_2^4}{\pi^5 |K|^2}$, $|K|^2 \doteq 0.93$ is the refractivity factor for water,

$\sigma(\lambda_2, D)$, in cm^2, is the backscattering cross section of a drop of

diameter D in cm, N (D,x), in $m^{-3} cm^{-1}$, is the DSD written as a function of

range and $Q_t(\lambda_1, D)$, in cm^2, is the total cross section. The limits on the

D integration are some assumed values D_{min} and D_{max}.

If the DSD is taken to be of the form

$$N(D, x) = N_0(x) \exp(-\bar{\Lambda} D) \quad (16)$$

where $\bar{\Lambda}$ is independent of range over the interval $r_k \leq x \leq r_j$, then a ratio

of the above equations is independent of N_0 (x) and can be solved for $\bar{\Lambda}$.

Writing $I(\bar{\Lambda}) = \int_D \sigma(\lambda_2, D) \exp(-\bar{\Lambda} D) dD$ then N_0 in the ith range bin, $k \leq i \leq j$,

can be found from the equation

$$N_{o,i} = \frac{r_i^2 \, P(\lambda_2, r_i)}{C_2 \, I(\bar{\lambda}) \, H} \qquad (17)$$

Assuming a drop velocity law, $v(D)$; then the rain rate at the ith bin becomes

$$R_i = 0.6\pi \, N_{o,i} \int_D D^3 v(D) \exp(-\bar{\lambda}D) \, dD \qquad (18)$$

The main drawbacks of this method are the overly restrictive assumption on the form of the DSD and the dependence of the estimated R on errors in the calibration constant. Since the interval attenuation is found via the Eccles and Mueller (1971) method, the error sources in A are the same as previously noted.

Over an interval of uniform rain rate, Goldhirsh and Katz (1974) were able to show that the two parameters of a mean DSD could be deduced for both attenuating/non-attenuating and dual attenuating wavelength combinations. To outline the latter method, it can be shown from the radar equation and the uniform rain rate assumption that

$$\frac{\log T_1}{\log T_2} = \frac{\int_{r_k}^{r_j} A_1(x)\,dx}{\int_{r_k}^{r_j} A_2(x)\,dx} = \frac{\int_D Q_t(\lambda_1, D) \exp(-\bar{\lambda}D)\,dD}{\int_D Q_t(\lambda_2, D) \exp(-\bar{\lambda}D)\,dD} \qquad (19)$$

where

$$T_i = P(\lambda_i, r_j)\, r_j^2 \Big/ P(\lambda_i, r_k)\, r_k^2 \qquad (20)$$

Notice that from the same set of measurables used in the Eccles and Mueller

(1971) approach a different equation is derived. This is a consequence of the uniform rain rate assumption. The parameter $\bar{\Lambda}$ can be found from this equation; $\bar{N}_o$ is obtained from the equation

$$\bar{N}_o = \frac{-5 \log T_i}{(r_j - r_k) \int_D Q_t (\lambda_i, D) \, exp(-\bar{\Lambda} D) \, dD} \tag{21}$$

where the subscript i can be set equal to either 1 or 2.

Error analyses of the method have been performed (Goldhirsh, 1975; Stogryn, 1975; Wexler, 1976). Essentially the dynamic range of the method is no less restrictive than the Eccles and Mueller approach. Moreover, the technique is limited to intervals along which the rain rate is nearly uniform. This is a more stringent requirement than the Eccles and Mueller assumption that the reflectivity factor is insensitive to wavelength. Nevertheless, this dual-wavelength technique offers the potential of measuring a two parameter DSD which is independent of the calibration constant. In this respect it appears to be unique among the dual-measurement techniques that have been proposed.

One of the first reports of experimental results on the dual wavelength method is by Kostarev and Chernikov (1968) who used wavelengths of 3 cm and 0.86 cm. The rain rate algorithm is essentially the same as that derived by Eccles and Mueller (1971). Comparisons were made between the average rain rates over a 2.88 km path as deduced by their dual wavelength method and by rain gages spaced 250 m apart. The authors

reported good agreement between the two sets of data when the rain rate is homogeneous over the interval. Inhomogeneous rain rates, however, often led to significant errors. The error was explained partly on the basis of unmatched antenna beamwidths; they reported improvements when the beams were matched in azimuth. Of course, other errors as discussed earlier must also have been operative.

Berjulev and Kostarev (1974) have reported additional measurements made by a 3.2 cm and 0.86 cm radar system. The path-integrated attenuations were compared to the same quantity deduced from the raingage data. For the 12 storms measured in 1969 the deviation between the measurements vary from 7.7% to 43.8% with an RMS error of 19.5%.

Yamada et al. (1978) have designed a dual-wavelength radar system that operates at 5 GHz and 14 GHz ($\lambda_2 = 6$ cm, $\lambda_1 = 2.14$ cm). Although their primary interest was in compiling cumulative statistics of the total path attenuation, they have also shown several individual graphs of the cumulative path attenuation (CPA) versus the range r. Despite the fact that the CPA must be a monotonically increasing function of range, the data indicate both small and very marked departures from this behavior. They note that the difference is probably not due to the unmatched antenna beamwidths and suggest possible effects of the frequency dependent reflectivities or rain depolarization. To these we should also add the possible influence of errors due to statistical fluctuations and, to account for the marked decrease in total attenuation, the possible presence of large, non-spherical drops or small wet hail (Eccles, 1979).

The results of Eccles (1979) have been referred to earlier. It is worth noting, especially in light of the regions of "negative" attenuations reported by Yamada et al. (1978), that the averaging and curve fitting technique of Eccles has been designed for the purpose of detecting hail (thereby identifying spurious regions of "negative" attenuation) and eliminating some of the statistical errors caused by insufficient sampling. The rather poor sensitivity of the S-band/X-band system employed restricts the method to cases of fairly long path intervals and to regions of moderate to heavy rain rates. For the twelve most intense storms which were analyzed, the rain rates deduced from the dual-wavelength method were in much better agreement with the rain gage estimates than those derived from a Z-R law using a single S-band radar. Despite these improvements, the discrepancies between the dual-wavelength and raingage estimates of path-averaged rainfall rate are significant. However, as noted in Section 5.2 and by Eccles, the gage predictions of rain rate over a path can be quite poor, especially for a sparsely distributed network. Thus, the technique is probably better than it appears.

Undoubtedly the most carefully conducted dual wavelength experiment performed to date is that of Joss et al. (1974). They used vertically pointing 0.86 and 5.6 cm radars, the latter with Doppler capability, five surface disdrometers and three rain gages all within a circle of radius of about 50 m. Extreme care was taken to average echoes and obtain best estimates of reflectivities from which to compute the 0.86 cm attenuation. Both radars were also calibrated by comparing the reflectivities at the

lowest range gate (580 m) with those computed from the surface DSD for the entire 2 1/2 hr test period. The differences in Z at 0.86 and 5.6 cm due to variations in DSD were within $\pm$ 1 db, but should be correlated in height, leaving a net expected error in differential attenuation of $\sim$ 0.5 db km^{-1}, which is reduced further with time integration. Using the DSD data and raindrop radar and attenuation cross-sections, they calculated the relation Z = 1360 $A^{1.38}$ [Z (mm^6 m^{-3}), A (db km^{-1})] as shown in Fig. 13.

The data points in Fig. 13 show that the measurements generally overestimated the DSD computed attenuation coefficients, the more so the smaller the reflectivity. This difference was attributed to contributions to attenuation but not to reflectivity by liquid water in cloud form. (short wavelength radiometer observations should be similarly affected.) They also found Doppler evidence of updrafts of $\sim$ 2.3 ms^{-1}, thus leading to enhanced attenuation aloft over that deduced from the surface DSD and gage data. This is consistent with our earlier explanations for the excessive attenuations measured by Semplak and Turrin (1969) and Anderson et al. (1947).

Important ancillary findings of Joss et al. (1974) relate to the sampling problems. They found that correlations between the radar measured log Z aloft and that computed from the ground DSD decreased sharply with increasing height as shown in Fig. 14. Even when adjusting for the lag at which the correlations were maximized, the standard deviation of the differences was 4 db between the surface and 1.22 km height. Without lag adjustment, it was 7 db. They also found an rms difference of 13% (i.e.,

1 db) between DSD Z's calculated from DSD data collected with disdrometers spaced only 100 m apart. This emphasizes what we have indicated earlier: that even modest displacement in space and time can lead to great differences between measurements which are expected to be well correlated. Indeed, the errors associated with spaced disdrometers and rain gages are usually sufficiently great to attribute much of the spread in scattergrams to those alleged "ground truth" instruments.

While Joss et al. (1974) did not use attenuation and reflectivity to deduce rainfall, their results are nevertheless highly relevant to this problem. In particular, reflectivity, attenuation, and rainfall are well correlated when proper account is taken of the sampling problems. But cloud water can affect 0.86 cm attenuation (and radiometry) at low rain rates and radar reflectivities.

The most comprehensive multi-parameter measurements made recently are those of Masuko et al. (1981). They used two scanning radars and radiometers operatings at wavelengths of 0.86 and 3.2 cm. The entire facility was installed in an airplane and flown over the ocean in trials of a simulated spaceborne rain measuring system. The antennas were either pointed toward the nadir or scanned over an angle of $\pm$ 23° perpendicular to the aircraft path.

In one mode, they compared the attenuation deduced from the 0.86 cm nadir reflection from the ocean by assuming a known surface reflection coefficient. The attenuation was then converted to rain rate assuming established relations. The 3.2 cm radar was used simultaneously to measure

the average Z below the bright band. Fig. 15 presents the data and the resulting relationship $Z = 126 R^{1.59}$, which is quite reasonable despite the slightly low coefficient. The downward looking radiometers measured brightness temperatures as shown in Fig. 16, also compared to the attenuation-deduced rain rates as described above. Of course, no rain gages were available on the ocean surface, but it is clear that the relations found are also reasonable. The correlation coefficient between the rain rate deduced from the 0.86 cm attenuation and the 3.2 cm brightness temperature is 0.91. However, the correlation with the 0.86 cm brightness temperature is only 0.67, probably because the shorter wavelength radiometer is affected by non-radar detectable cloud liquid water. Of course, at vertical incidence in stratiform rain it is not unreasonable that the total path attenuation from the 0°C level down should be consistent with the radar reflectivity below the 0°C level since the rain is probably vertically homogeneous. On the other hand, errors might be expected at the lower rain rates because of the excess attenuation through the bright band. In any case, the results show promise for the three methods (i.e., radar, path attenuation, and radiometry) although the latter two are proxies for one another.

5.3.2 Dual Polarization Methods

In 1976 Seliga and Bringi proposed a dual polarization technique from which a two parameter exponential drop size distribution could be obtained. The suggested measuring instrument was an incoherent S-band radar with the

capability of measuring the co-polarized return powers along the horizontal, P_h, and vertical, P_v, directions. The method has since been used both in estimating the DSD and in discriminating rain from hail (e.g., Cherry et al., 1980); in this discussion only the former will be dealt with.

It should be noted that it is probably Barge (1972, 1974) who should be credited with the concepts which triggered the work of Seliga and Bringi (1976) for it was he who first showed that the cancellation depolarization ratio (CDR) was correlated with rain rate. He correctly attributed this to the increasing number of large oblate raindrops accompanying increasing rain rates. However, Humphries (1974) found that the CDR was contaminated by depolarization in the intervening rainfall. It was then that Seliga and Bringi conceived of using orthogonal linear polarizations from which sufficient information could be obtained to deduce the DSD parameters.

The basic idea of the technique is that the ratio P_h/P_v is independent of the multiplicative factor N_0 of the DSD; therefore the slope Λ of the exponent can be determined. N_0 is then deduced from either P_h or P_v.

Explicitly, from the radar equation and from the definition of Z,

$$P_q(r_j) = \frac{C_q Z_q(r_j)}{r_j^2} = \frac{H C_q}{r_j^2} \int_D \sigma_q(D) N(D)\, dD \qquad (22)$$

where $\sigma_q(D)$ in cm^2 is the backscattering cross section of a drop whose volume equals that of a sphere of diameter D. The subscript $q = \{h,v\}$ refers to an incident and backscattered field polarized along the q

direction. To write Z_q in the form above requires the use of several assumptions that are discussed below.

Using Eq. (1) with $\Lambda = 3.67/D_o$ it follows that $Z_{DR} = 10 \log (Z_h/Z_v)$ where

$$\frac{Z_h}{Z_v} = \frac{C_v \, P_h}{C_h \, P_v} = \frac{\int_D \sigma_h (D) \exp(-\Lambda D) dD}{\int_D \sigma_v (D) \exp(-\Lambda D) \, dD} \quad (23)$$

From knowledge of C_h/C_v and $\sigma_q(D)$, one can solve for Λ and D_o since the right hand side of Eq. (23) is a function of D_o only. The behavior of Z_{DR} and Z_h/N_o as functions of D_o is shown in Fig. 17. After determining D_o, N_o is then computed from the equation

$$N_o = \frac{r_j^2 \, P_q(r_j)}{H \, C_q \int_D \sigma_q (D) \exp(-\Lambda D) \, dD} \quad (24)$$

In contrast to the dual wavelength method which can be applied only over an interval (usually longer than the range resolution), potentially the dual polarization method can be used at each range bin. An obvious advantage of a method which provides an estimate of the DSD from measured quantities is that it does not require an empirical law to relate radar and meteorological quantities. For the determination of liquid water content or rain rate the success of the method is largely dependent on how accurately the DSD can be determined.

Seliga and Bringi (1978) listed a number of possible error sources in

the method. Since then many experimental studies and error analyses have been carried out. What follows is a brief discussion of the major errors in the method and a summary of some of the relevant work.

It is evident from the manner in which Λ and N_o are determined that both C_h/C_v and either C_h or C_v must be assumed. Since a single antenna is used to measure P_h and P_v, C_h/C_v generally can be determined more accurately than C_h or C_v alone. Of course, the errors in these quantities can be minimized by standard calibration methods, by in-situ calibration using rain gages and disdrometers (Browning, 1978) and by procedures for calibrating the $Z_{DR} = 10 \log (Z_h/Z_v)$ measurements (Seliga et al., 1981). Another possibility is to find another measurable that is independent of the absolute calibration constant. Generally, such measurement schemes are not dual polarization methods in the normal sense of the word.

Since the method offers two measurements, only a two parameter DSD can be specified. Moreover, the D_{min} and D_{max} limits of integration must be assumed. Cherry et al (1979), Hall et al. (1980a) and Ulbrich and Atlas (1982a) have studied the effect of D_{max} on the Z_{DR} measurement, showing that the latter is sensitive to D_{max} when the median equivalent volume diameter is greater than about 0.2 cm. However, if $D_{max}/D_o > 2.5$ then the dependence of Z_{DR} on D_o is essentially independent of variations in D_{max}. Ulbrich and Atlas have also shown that if the three parameters of a gamma DSD could be obtained, the improvement in the method would be substantial. To obtain the additional measurement required, the use of path integrated microwave or optical attenuation has been suggested (see Section 4).

It was noted earlier that several assumptions must be made in order to express the reflectivity factor as the product of $\sigma_q(D)$ and $N(D)$ integrated over the equivalent volume diameter D. For a more general assemblage of particles, this single integral would be replaced by integrations over density, size, shape and orientation angles of the particles. To reduce this multiple integration to a single integration it is first assumed that the rain drops are oblate spheroids with a one to one correspondence between D and the ratio of the minor to major axis of the particles (Pruppacher and Beard, 1970; Green, 1975). Secondly, it is assumed that the fluctuations of the angle of orientation of the minor axis about the vertical are sufficiently small that the rain drops may be assumed to be aligned along a common direction (Seliga and Bringi, 1978). This preferred orientation of rain drops is, in fact, the main basis of distinguishing liquid from solid hydrometeors (Cherry et al., 1980; Hall et al., 1980b). Several studies of particle shapes have been made (Bringi and Seliga, 1977a, 1977b; Seliga and Bringi, 1977). The effects of drop canting angle have also been investigated, but to our knowledge none have been used to translate such effects into errors in the Z_{DR} method. A final error source is due to the finite number of independent samples at each polarization. To reduce sampling errors, P_h and P_v should be staggered with a brief time interval between them and a much longer time interval between each P_h, P_v pair. In this way successive P_h, P_v measurements are highly correlated while each P_h, P_v pair is nearly decorrelated with all others (Bringi et al., 1978). Under this situation standard errors in Z_{DR} of about 0.075 db can be made with about 50 independent P_h or

P_v samples (Hall et al., 1980a). There are also different ways of forming the Z_{DR} ratio. Bringi et al. (1980) has shown that an average of the form $\langle Z_{DR} \rangle = 10 \log (\langle P_h \rangle / \langle P_v \rangle)$ (where the angular brackets denote a sample mean over the received pulses) is asymptotically unbiased and has the smallest standard deviation among the estimators which are possible.

Despite the number of potential error sources in the technique, the experimental results have been very encouraging. Basically, four kinds of comparisons have been made between meteorological parameters derived from the Z_{DR} method and the same parameters measured by more direct means. Using a relationship for attenuation A, in terms of N_o and D_o, the Z_{DR} method was used to compute values of N_o, D_o and then values of A at each range bin (Hall et al., 1980c). Summing the estimated values of A along the path of an 11.6 GHz satellite downlink provides an estimate of the path integrated attenuation with which the directly measured attenuation can be compared. For the rather small values of attenuation which were measured, agreement between the two sets of attenuation versus time curves is quite good, exhibiting a standard deviation of about 0.3 db as shown on the left of Fig. 18. In contrast, the attenuation found from an A-Z relation, derived by assuming a Marshall-Palmer DSD, was in error by about a factor of two. The agreement between directly measured attenuation and that deduced from raingage data was even poorer (Fig. 18, right side).

In an experiment using the CHILL radar (Seliga et al., 1981), rain rates derived from the Z_{DR} technique were compared against rain gage measurements. The agreement between these sets of rain rates were

significantly better than comparisons with the rain rates deduced by means of a Z-R law. This held true even when a rain gage calibration method was used along with the Z-R method.

Another experiment using the CHILL radar and a disdrometer has been reported (Seliga et al., 1980). For this case, the temporal record of the disdrometer was used to reconstruct the range-profiled rain rate by means of an estimate of the storm speed. Again, the Z_{DR}-derived R compared more favorably with the disdrometer-derived R than did the R estimated from Z alone.

A more direct comparison between quantities measured by a radar and a disdrometer has been given by Goddard et al. (1982). In that experiment, the radar measured values of $Z_{DR} = 10 \log (Z_h/Z_v)$ and Z_h were compared to the values derived from a disdrometer. The conversion of disdrometer data to the radar quantities, Z_{DR}, Z_h enabled them to dispense with any apriori assumption concerning the DSD. They found that the radar measured Z_{DR} was on the average 0.3 db smaller than that deduced from the disdrometer, while the radar measured Z_h exceeded the disdrometer estimate by 1.6 db. The authors note that although the Z_h discrepancy can be explained on the basis of disdrometer errors, this is not the case with the Z_{DR} estimates. To reduce the bias in radar measured Z_{DR}, the relationship between D and the ratio of minor to major axes of the oblate spheroid is modified so that, in effect, the smaller drops are taken to be more spherical in shape than would be predicted from the equilibrium results of Pruppacher and Beard (1970). This modification reduces the Z_{DR} bias to 0.15 db while having a

negligible effect on Z_h. A partial justification for this procedure is found in the experimental data of Jameson and Beard (1982), although the data suggest shapes that are more nearly spherical than those of drops in equilibrium at larger values of D as well. Other possible errors sources are the effects of canting angle, unequal sampling volumes of the radar and disdrometer, and the time lag caused by the spatial separation (120 m) between the sampling volumes.

In another recent paper, Stickel and Seliga (1981) report on estimates of D_o and W (liquid water content) made by both in-situ measurements using Knollenberg (1976) probes and by means of the Z_{DR} method. Excellent agreement was found between the two D_o values, but the Z_{DR} method provided a value of W which was about a factor of 10 less than the in-situ measurement. The authors explain the source of discrepancy as due to an error in the radar calibration constant.

5.4 Range-Profiling Algorithms

There are several cases of interest in which the following situation arises: we have available the attenuated radar return powers at each range gate as well as an estimate of the total path attenuation (taken at the same wavelength and along the same path) and we wish to determine the rain rate along the range direction. These are the data that are obtained, for example, in the fixed target method and in the radar/radiometer and radar/satellite downlink combinations (see Section 5.2). For the latter two sensors it is assumed that the wavelengths are identical.

According to the hypothesis, the total path attenuation, $\overline{AL}$, can be estimated, where

$$\overline{AL}_\nu = \int_0^{L_\nu} A(x)\, dx \tag{25}$$

The path length L_ν is equal to νh, where ν is the total number of range gates and h is the range resolution.

A second estimate of this quantity can be obtained by means of a method first derived by Hitschfeld and Bordan (1954). They have shown that for an attenuating wavelength radar, the rain rate at the jth bin, R_j, can be expressed as a function of the return powers $P(\lambda_i, r_k)$ ($k = 1, ..., j$), C_i, the radar constant for wavelength λ_i, and the parameters in the $A = \xi Z^\beta$ and $R = aZ^b$ laws. Assuming that a, b, ξ, and β are independent of range, then we can write this solution in the form

$$R_j = a\left[\frac{P(\lambda_i, r_j)\, r_j^2}{C_i}\right]^b f_j^b \quad ; \quad j = 1, 2, \cdots, \nu \tag{26}$$

where

$$f_j = \left[1 - 0.46\,\xi\beta h \sum_{k=1}^{j} \epsilon_{kj}\left(\frac{P(\lambda_i, r_k)\, r_k^2}{C_i}\right)^\beta\right]^{-\frac{1}{\beta}} \tag{27}$$

where

$$\epsilon_{kj} = 1 \text{ for } k \neq j \quad \text{and} \quad \epsilon_{kj} = 0.5 \text{ for } k = j$$

From the radar equation and the expression for R_j, we can infer the path-integrated attenuation out to the jth range bin ($j \leq \nu$). This is simply

$$\bar{A} L_j = 5 \log f_j \quad where \quad L_j = j\hbar \tag{28}$$

By letting j increase to ν, a second estimate of the total path-integrated attenuation is obtained, i.e.,

$$(\bar{A} L_\nu)' = 5 \log f_\nu \tag{29}$$

where f_ν is given by Eq. (27) with j replaced by ν. In general $(\bar{AL}_\nu)'$, which is determined from the return powers from the individual range gates, is not equal to $\bar{AL}$ of equation (25) which is found by means of a path-integrated measurement. However, by adjusting ξ, β, or C_i in the expression for f_ν, we can insure the agreement between the two. The parameters so determined can then be inserted into Eq. (26) which yields the range profiled rain rate. Details of this algorithm are given in Meneghini et al. (1982).

A simple error analysis of this method has been carried out (Meneghini et al., 1982). It was shown that an adjustment of the calibration constant C_i leads to range profiled rain rates that are independent of errors in the calibration constant and in the Z–R and A–Z laws, but dependent on the A–R

law and errors in the path-integrated attenuation measurement. In the analysis, however, it was assumed that the R-Z and A-Z relationships were constant along the entire path. Although a and ξ were treated as randomly varying from path to path, the parameters b and β were assumed to be constant and unbiased.

A somewhat different approach to this problem has been given by Lu (1980). Although the method was developed for a radar/radiometer sensor pair, it can be applied unchanged to the other measurement systems cited above.

From the radar equation and an $A = \xi\, Z^{\beta}$ law, we can write

$$A_1 = \xi\, Z_1^{\beta} = \xi \left(\frac{P(\lambda_i, r_1)\, r_1^2}{C_i} \right)^{\beta}$$

$$A_2 = \xi\, Z_2^{\beta} = \xi \left(\frac{P(\lambda_i, r_2)\, r_2^2}{C_i} \right)^{\beta} e^{\beta h A_1}$$

$$\vdots$$

$$\text{(30)}$$

$$A_\nu = \xi\, Z_\nu^{\beta} = \xi \left(\frac{P(\lambda_i, r_\nu)\, r_\nu^2}{C_i} \right)^{\beta} e^{\beta h (A_1 + A_2 + \cdots + A_{\nu-1})}$$

where the exponent of the ith equation is found from the previous (i-1) equations. These equations are now subjected to the constraint that the radar path integrated attenuation $\overline{AL} = h\,(A_1 + \ldots + A_{\nu-1})$ be equal to the path integrated attenuation derived from the radiometric intensity

measurement, τ_p. That is,

$$\tau_p = h\left(A_1 + A_2 + \cdots + A_{\nu-1}\right) \tag{31}$$

This constraint allows us to vary either ξ or β in the above equations until this equality is satisfied. This being accomplished, the sets of $\{A_i\}$ and $\{Z_i\}$ quantities follow immediately.

It should be noted that the first to propose a technique of this type were Hitschfeld and Bordan (1954). They suggested that the parameters in the rain rate estimate could be adjusted so that agreement was obtained between this and a rain gage reading deep in the storm. This method serves to bound the errors in the rain rates determined up to that point. In essence, the only difference between their method and the others here described is that a different measurable is used as a constraint.

Finally, it should be mentioned that methods of this type may be of some use in the context of the dual attenuating/non-attenuating wavelength method. Since the interval attenuation is monotonically increasing function of the interval length, it follows that the fractional standard deviation of this quantity will generally decrease with increasing path length. For a variety of situations, this interval may be comprised of many adjacent range gates. Under these circumstances, it is not difficult to show that with minor changes in the range profiling algorithms described above, the rain rates can be estimated at each range gate within the interval of interest.

6. Some Inferential Methods

While it would be desirable to develop a remote measurement scheme which could be completely automated, we recognize that at least for the time being, human intervention can often greatly enhance the accuracy of measurements. For example, the use of a Range Height Indicator (RHI) display provides a wealth of information concerning the horizontal and vertical homogeneity of the rainfall, the vertical gradients of reflectivity due to growth, evaporation, or wind shear drop size-sorting, or as a result of displacement of the rain streamers out of the plane of observation due to cross winds. All of these features relate to both errors in sampling at the surface and to ways of correcting surface measurements for such effects.

It is also clear that in the case of stratiform rainfall, considerable information about the nature of the DSD and precipitation rate is contained in the reflectivity profile across the bright band (BB). Until now, this information has not been exploited because we have lacked adequate vertical resolution to view the BB from the side. However, theoretical studies of the evolution of the DSD and the accompanying Doppler spectra across the melting layer by Ekpenyong and Srivastava (1970) suggest that the depth of the BB is sensitive to both the median volume particle size as well as to the precipitation rate, assuming no complexities associated with aggregation or breakup. While the absolute depth of the BB also depends upon the temperature lapse rate within the melting layer, the depth of the

BB may be defined by the layer encompassed within the two -6 db points above and below the height of the maximum reflectivity. While it is generally acknowledged that the depth of the BB increases with precipitation rate, at least to rates of about 10 mm/hr (which is very high for stratiform precipitation in any case), we know of no attempts to use that as a measure because of the inadequate resolution of most radars. However, it should not be overlooked at least as a qualitative indicator with high resolution radars or at vertical incidence where high resolution may be achieved with short pulse lengths.

Another BB indicator of precipitation intensity which must be considered qualitative for the time being is the ratio of the peak reflectivity of the BB, η_p, to that above, η_a, and/or below, η_b. The ratio η_p/η_a should increase with precipitation rate because the rate of snow crystal aggregation increases with the precipitation rate. Similarly, the greater the aggregation, the greater the breakup, and thus the larger the ratio η_p/η_b. While these relationships have been noted qualitatively, we are unaware of any quantitative studies which demonstrate them clearly.

Many years ago it was also noted (Newell et al., 1957) that the circular depolarization ratio (CDR) was often much smaller in the melting layer than in either the snow above or the rain below. This was attributed to both the flatness of the snowflake aggregates and their tendency toward horizontal orientation as anticipated by Atlas et al. (1953). With the advent of the dual polarization differential reflectivity (ZDR) method, similar results have again been reported in the BB (Hall et al., 1980b).

It is also pertinent to note that Cherry et al. (1979) have noted that the ZDR peaks at a height a few hundred meters below the peak of the BB; indeed, it appears to occur near the height where the reflectivity itself has attained the value corresponding to rain. They attribute this to the large differential polarization effects of oriented wet flakes much as described above. But, in order that the peak of the BB differ so much from that of ZDR, it seems clear that the particle size weighting of the reflectivity must differ markedly from that for ZDR. The suggestion is, therefore, that the peak ZDR occurs essentially just above the level at which the largest particles in the size spectrum melt completely. If this is correct, then the difference in height between the peaks in Z and ZDR should be a measure of the breadth of the particle size distribution. Evidence in support of this contention should be attainable from high resolution vertically pointing Doppler measurements.

It would thus appear that the combination of the reflectivity ratios across the bright band and ZDR measurements should also be at least a qualitative indicator of aggregation, breakup, size spectrum breadth, and of rain intensity. This can readily be determined by correlating either CDR and ZDR in the BB to Z and or rain rate below; similar correlations should be sought with the depth of the layer between the peak Z and ZDR.

Another feature which should be explored is the effect of size sorting due to wind shear on the drop size spectrum, Z, and ZDR. Gunn and Marshall (1955) have modeled and Atlas and Plank (1953) have observed the history of the DSD, reflectivity, and rain rate due to wind shear. When precipitation

generating cells are sufficiently far apart, it is well known that the initial drops to reach the surface at the leading edge of the cell are the largest and thus produce Z's larger than expected with unsorted DSD's of the same rain rate; the converse is true at the trailing edge. Effects such as these account for much of the scatter about the mean Z-R regression relationship, and indeed, also for systematic shifts in the Z-R relation on the rain a parameter diagram. Examination of high resolution RHI displays of Z and ZDR by the first of us (private communication with S. M. Cherry, 1981) has shown evidence of drop size sorting. Because much of the theory on which the ZDR method is based assumes an exponential DSD, observations such as these should permit the determination of when such an assumption is valid and the development of correction algorithms for use when it is not.

Finally, while this work has concentrated entirely on rainfall, a few words are in order concerning the discrimination of rain from hail. It is apparent from the RHI profiles of reflectivity factor and differential reflectivity presented by Hall et al. (1980b) that the combination of these two measurables can be used to distinguish rain from hail or water-coated ice particles. Although a quantitative, automatic method for identifying hydrometeor type using these measurables has not yet been established, the method shows promise. This is particularly true when the measurements are combined with subjective criteria by the observer.

Another multi-parameter method for identification of hail is the dual-wavelength hail detection scheme of Eccles and Atlas (1973) referred to in Section 5. The usefulness of the technique has been investigated by

Srivastava and Jameson (1977) who suggest that the ratio of the reflectivity factors at two wavelengths is a better measure o `hydrometeor type. The latter method has been further investigated by Ullrich and Atlas (1982b) and implemented for Colorado hailstorms by Jameson and Heymsfield (1980). This method also not yet been developed fully so that automatic identification of hydrometeor type and size can be made.

7. Summary and Conclusions

In this paper we have attempted to review the rationale behind the use of multi-parameter observations aimed at rainfall measurements of improved accuracy. We simulate the potential improvements attainable with various combinations of remote measurables, discuss the various concepts proposed, and review those experiments which have been attempted for these and related purposes.

In Section 2 we summarize t.e long history of Z-R and drop size distribution (DSD) measurements which finally led to the conclusions that radar rainfall relationships suffered from both systematic variations and scatter due to deviations in the drop size and number from well established DSD's such as that due to Marshall and Palmer (1948). To overcome this problem Atlas and Chmela (1957) developed a rain parameter diagram which required the specification of two parameters. Ulbrich and Atlas (1978) extended that diagram by adding several other parameters including microwave and optical attenuation, but requiring the DSD to be exponential. The use of the latter rain diagram by Ulbrich and Atlas (1982a) showed that

the accuracy of rain rate specification could be improved significantly by the use of a third variable which accounted for the breadth of the distribution. This was done through the use of a gamma DSD. Accordingly, in the present paper (Section 3), we generalize the Ulbrich-Atlas rain parameter diagram still further.

In Section 4 we use DSD's to compute or simulate the remotely measurable parameters reflectivity, Z, specific attenuation, A, optical extinction, Σ, and differential reflectivity, Z_{DR}, and the rain rate, R, and median volume diameter, D_o. We then demonstrate that R calculated from pairs of remotely measured parameters such as (Z, A) or (Z, Σ) decreases the errors by factors of about 6 and 4, respectively. Finally, the use of three parameters (Z, Z_{DR}, Σ) produces virtually perfect agreement. While these simulations indicate the considerable potential value of the use of multiple parameters, they fail to simulate the various sources of error in the actual measurement systems.

The remainder of the paper is devoted to a review of the various remote measurement concepts and illustrative experiments which demonstrate their capabilities and limitations. We focus first on path-average microwave attenuation. Despite the disappointing agreement between most experimental attenuation measurements and the theoretical values expected from surface rain gage data which disturbed Medhurst (1965), we agree with Hogg and Chu (1975) that most of the errors are due to rain gage sampling problems and to vertical air motions which produce differences between the rain rates in the elevated paths and at the level of the gages. When these

problems are eliminated as in the well designed 35 GHz experiment of Norbury and White (1972), excellent results are found, so much so, that we believe that a similar system modified to cover an area of some 100 m on a side would be far superior to any presently conceivable raingage system.

We also emphasize that the sampling and vertical air motion problems which have plagued the above experiments also account in large part for much of the discrepancies in radar-rainfall experiments. In short, there is considerable doubt about the "truth" of rain gages.

It is also shown that passive microwave radiometry is a fine proxy for path integrated attenuation up to values of about 10 db. It has the great advantage of not requiring either a reflector or receiver at the end of the path, thus allowing measurements from a single site, or even with the same antenna as may be used for simultaneous radar measurements. However, in order to achieve sufficient dynamic range one must use a multiplicity of wavelengths. Radiometric measurements of path average rainfall by Lu (1980) show good agreement with gage values.

The availability of stable microwave beacons on communications satellites has opened the door to their use in path attenuation measurements. Moreover, the need for rainfall and attenuation statistics for earth-space communications has given new impetus to the development of a variety of schemes to obtain proxy attenuation data from weather radars and radiometers. Various investigators have used radar-rainfall and attenuation-rainfall relations to transform radar measurements to path attenuation. Very good agreement has been found in this way except when

the radar beam traverses the bright band or hail. Agreement is improved further when the basic relationships are adjusted for the actual DSD below the path. Similarly good agreement has been found between radiometer-deduced and actual attenuation.

In the area of optical extinction surprisingly little has been done since the early predictions of Atlas (1953). One very well done experiment by Chu and Hogg (1968) finds good agreement between their measurements and the empirical findings of Atlas (1953). The disadvantages are that it is restricted to short paths and, in the case of light rain, may be affected by fog, dust, and/or pollution.

We then proceed to the variety of dual wavelength and dual polarization (Z_{DR}) techniques which have been treated in radar meteorology. For a variety of reasons including excessive signal fluctuations, difference in reflectivity and/or unmatched beams at the two wavelengths, non-Rayleigh scatterers such as hail, and the modest attenuation at some wavelengths and small rain rates, the methods have not produced very promising results over short paths. However, Eccles (1979) appears to have achieved reasonable success in using the method over a larger range azimuth domain in comparison to cumulative rainfall measured by a 1600 km^2 surface network of gages. In essence, however, we believe that the method reduces to a path averaged measurements technique. A variant on the above is the method of Goldhirsh and Katz (1974) which assumes a uniform rainfall rate over some path to arrive at the effective exponential DSD. The requirement for a uniform rain rate is surely too stringent except in steady stratiform

precipitation.

While the work of Joss et al. (1974) was not aimed at evaluating the dual wavelength method, it did demonstrate that reflectivity, attenuation, and rainfall rate are highly correlated when proper account is taken of the sampling problems. But undetected cloud water can produce excessive attenuation at short wavelengths at small rain rate and reflectivity. The most exciting recent multi-parameter experiment is that of Masuko et al. (1981) who used radars and radiometers at 0.86 and 3.2 cm in an airborne laboratory. Using the 0.86 cm radar in a nadir reflection mode from the sea, they measured attenuation. The rainfall deduced thereby was well correlated with the 3.2 cm reflectivity below the melting level and with the radiometric brightness temperatures at both wavelengths.

Dual wavelength techniques and radiometric methods are more promising when they are used to estimate attenuation. The latter is then used as a constraint on the retrieval of range profiled rain rates from the radar measurements. The best results in gate-by-gate measurements have been achieved with dual polarization or differential reflectivity (Z_{DR}). However even these have failed to meet their full potential because rainfall often does not behave according to the apriori assumptions. An accompanying paper (Ulbrich and Atlas, 1982a) shows that the use of a third remote parameter in addition to Z and Z_{DR} offers great promise.

In many cases, accuracy can be greatly enhanced and ambiguities resolved by personal examination of the radar displays which depict the nature of the bright band, cell spacing, homogeneity, and drop size sorting

effects.

One very important field of multi-parameter measurement techniques which has not been covered in depth in this review is that which includes polarization diversity methods other than those discussed in this work in connection with Z_{DR}. The use of polarization methods for the measurement of precipitation is covered in a paper by Humphries and Barge (1982) to be presented at this symposium. The methods are not sensitive to canting Z_{DR} methods and have therefore been used primarily as a means of identifying hydrometeor type. However, recent work which has been directed toward relating polarization diversity effects to rainfall parameters and other precipitation characteristics indicates that the methods have considerable promise.

With a growing appreciation of the needs and the capabilities of the various techniques and growing evidence of the willingness to invest the necessary effort and resources to do the job right, the outlook for highly improved remote rainfall measurements seems bright.

Acknowledgements

REFERENCES

Anderson, L. J., J. P. Day, C. H. Freres and A. P. D. Stokes, 1947: Attenuation of 1.25-centimeter radiation through rain, Proc. IRE, 35, 351-354.

Atlas, D., 1947: Preliminary report on new techniques in quantitative radar analysis of rainstorms. Rept. ANMW 7-4, pt. I. Dayton, Ohio: AMC, Wright-Patterson AFB.

Atlas, D., 1948: Some experimental results of quantitative radar analysis of rainstorms. Report ANMW 7-4, pt. II. Dayton, Ohio: AMC, Wright-Patterson AFB.

Atlas, D., 1953: Optical extinction by rainfall. J. Meteor., 10, 486-488.

Atlas, D., 1954: The estimation of cloud parameters by radar. J. Meteor., 11, 309-317.

Atlas, D., 1964: Advances in radar meteorology. Adv. Geophys., 10, 317-478.

Atlas, D., and Chmela, A. C., 1957: Physical-synoptic variations of drop-size parameters. Proc. Sixth Wea. Radar Conf., Amer. Meteor. Soc., Boston, pp. 21-30.

Atlas, D., and F. Ludlam, 1961: Multi-wavelength radar reflectivity of hailstorms. Quart. J. Roy. Meteor. Soc., 87, 523-534.

Atlas, D., and V. G. Plank, 1953: Drop-size history during a shower. J. Meteor., 10, 291-295.

Atlas, D., and C. W. Ulbrich, 1974: The physical basis for attenuation-rainfall relationships and the measurement of rainfall parameters by combined attenuation and radar methods. J. Rech. Atmos., 8, 275-298.

Atlas, D., and C. W. Ulbrich, 1977: Path- and area-integrated rainfall measurement by microwave attenuation in the 1-3 cm band. J. Appl. Meteor., 16, 1322-1331.

Atlas, D., M. Kerker, and W. Hitschfeld, 1953: Scattering and attenuation by non-spherical atmospheric particles. J. Atmos. Terres. Phys., 3, 108-119.

Austin, P. M., 1947: Measurement of approximate raindrop size by microwave attenuation. J. Meteorol., 4, 121-124.

Austin, P. M., and R. Richardson, 1952: A method of measuring rainfall over an area by radar. Proc. 3rd Weather Radar Conf., McGill University, Montreal, pp. D13-D20.

Austin, P. M., and E. L. Williams, 1951: Comparison of radar signal intensity with precipitation rate. Weather Res. Tech. Rept. no. 14, Cambridge, Mass.: Dept. of Meteor., MIT.

Barge, B. L., 1972: Hail detection with a polarization diversity radar. Sci. Rep. MW-71, Stormy Weather Group, McGill University, Montreal, 80 p.

Barge, B. L., 1974: Polarization measurements of precipitation backscatter in Alberta. J. Rech. Atmos., 8, 163-173.

Bartnoff, S., and D. Atlas, 1951: Microwave determination of particle size distribution. J. Meteor., 8, 163-173.

Battan, L. J., 1973: Radar Observation of the Atmosphere, University of Chicago Press, Chicago, 324 pp.

Berjulev, G. P., and V. V. Kostarev, 1974: Dual wavelength radar measurements of 8 mm radiowave attenuation by atmospheric precipitation and clouds. J. Rech. Atmos., 8, 358-363.

Best, A. D., 1950: The size distribution of raindrops. Quart. J. Roy. Meteor. Soc., 76, 16-36.

Blanchard, D. C., 1953: Raindrop size distributions in Hawaiian rains. J. Meteor., 10, 457-473.

Bringi, V. N., and T. A. Seliga, 1977a: Scattering from non-spherical hydrometeors. Proc. URSI Open Symposium on Propagation in Non-Ionized Media, La Baule, France, pp. 199-204.

Bringi, V. N., and T. A. Seliga, 1977b: Scattering from axisymmetric dielectrics or perfect conductors imbedded in an axisymmetric dielectric. IEEE Trans. Ant. Prop., AP-5, 575-580.

Bringi, V. N., S. M. Cherry, M. P. M. Hall, and T. A. Seliga, 1978: A new accuracy in determining rainfall rates and attenuation due to rain by means of dual-polarization radar measurements. IEE Conf. Proc., No. 169, Part II, Antennas and Propagation. London, England, 28-30 Nov. pp. 120-124.

Bringi, V. N., T. A. Seliga, and M. G. SriRam, 1980: Statistical characteristics of the differential reflectivity radar signal. Preprints 19th AMS Conf. on Radar Meteorology, Amer. Meteor. Soc., Boston, pp. 692-696.

Browning, K. A., 1978: Meteorological aspects of radar. Rept. Prog. Phys., 41, 761-806.

Brussaard, G., 1981: Prediction of attenuation due to rainfall on earth-space links, Radio Science, 16, 745-760.

Carbone, R. E., 1972: Evaluation of a dual-wavelength hail detector. Proc. 15th AMS Conf. on Radar Meteorology, Amer. Meteor. Soc., Boston, pp. 7-12.

Cataneo, R., 1969: A method for estimating rainfall rate-radar reflectivity relationships. J. Appl. Meteor., 8, 815-819.

Cataneo, R., and G. E. Stout, 1968: Raindrop-size distributions in humid continental climates, and associated rainfall rate-radar reflectivity relationships. J. Appl. Meteor., 7, 901-907.

Cherry, S. M., J. W. F. Goddard, M. P. M. Hall, and G. R. Kennedy, 1979: Measurement of raindrop-size distributions using dual-polarization radar. Proc. 5th Int. Conf. on Erosion by Solid and Liquid Impact, Cambridge, UK, pp. 18-2 to 18-7.

Cherry, S. M., J. W. F., Goddard and M. P. M. Hall, 1980: Examination of raindrop sizes using a dual-polarization radar. Proc. 19th AMS Conf. on Radar Meteorology, Amer. Meteor. Soc., Boston, pp. 526-531.

Chu, T. S., and D. C. Hogg, 1968: Effects of precipitation on propagation at 0.63, 3.5, and 10.6 microns. Bell Sys. Tech. J., 47, 723-759.

Collis, R. T. H., 1961: Digital processing of weather radar data. Proc. 9th Wea. Radar Conf., Amer. Meteor. Soc., Boston, p. 371.

Cox, D. C., 1981: Depolarization of radio waves by atmospheric hydrometeors in earth-space paths: A review. Radio Science, 16, 781-812.

Donnadieu, G., 1980: Observation de 2 changements rapides et importants das spectres des gouttes de pluie dans une averse issue de nuages stratiformes. (Submitted to J. Rech. Atmos.; private communication.)

Eccles, P. J., 1975: Ground truth tests of the dual-wavelength radar detection of hail. Preprints 16th AMS Conf. on Radar Meteorology, Amer. Meteor. Soc., Boston, pp. 41-42.

Eccles, P. J., 1979: Comparison of remote measurements by single- and dual-wavelength meteorological radars. IEEE Trans. Geosci. Elec., GE-17, 205-218.

Eccles, P. J., and D. Atlas, 1973: A dual-wavelength radar hail detector. J. Appl. Meteor., 12, 847-856.

Eccles, P. J., and E. A. Mueller, 1971: X-band attenuation and liquid water content estimation by a dual-wavelength radar. J. Appl. Meteor. 10, 1252-1259.

Ekpenyong, B. E., and R. C. Srivastava, 1970: Radar characteristics of the melting layer--A theoretical study. Unpub. Technical Report No. 16, University of Chicago, Lab. for Atmos. Probing.

European Space Agency, 1977: ATS-6 propagation experiments in Europe. Proc. of meeting held at ESTEC, Noordwijk, Netherlands, Sept. 6-7, ESA SP-131.

Fedi, F., 1981: Prediction of attenuation due to rainfall on terrestrial links. Radio Science, 16, 731-744.

Foote, G. B., 1966: A Z-R relation for mountain thunderstorms. J. Appl. Meteor., 2, 229-231.

ᵀujita, T. T., 1981: Tornadoes and downbursts in the context of generalized planetary scales. J. Atmos Sci., 8, 1511-1534.

Godard, S., 1965: Proprietes de l'attenuation par las pluie des ondes radioelectriques dan la bande 0.86 cm. J. Rech. Atmos., 2, 121-167.

Goddard, J. W. F., S. M. Cherry, and V. N. Bringi, 1982: Comparison of dual-polarization radar measurements of rain with ground-based disdrometer measurements. J. Appl. Meteor., 21, 252-256.

Goldhirsh, J., 1975: Improved error analysis in estimation of raindrop spectra, rain rate and liquid water content using multiple wave-length radars. IEEE Trans. Ant. Prop., AP-23, 718-720.

Goldhirsh, J., 1976: Attenuation of propagation through rain for an earth-satellite path correlated with predicted values using radar. IEEE Trans. Ant. Prop., AP-24, 800-866.

Goldhirsh, J., and I. Katz, 1974: Estimation of raindrop size distribution using multiple wavelength radar systems. Radio Science, 9, 439-446.

Green, A. W, 1975: An approximation for the shapes of large droplets. J. Appl. Meteor., 14, 1578-1583.

Gunn, K. L. S., and T. W. R. East, 1954: The microwave properties of precipitation particles. Quart. J. Roy. Meteorol. Soc., 80, 522-545.

Gunn, K. L. S., and J. S. Marshall, 1955: Effect of wind shear on falling precipitation. J. Meteor., 12, 339-349.

Hall, M. P. M., S. M. Cherry, and J. W. F. Goddard, 1980a: Use of dual-polarization radar to measure rainfall rates and distinguish rain from ice particles. IEEE International Radar Conference, Washington, DC.

Hall, M. P. M., S. M. Cherry, J. W. F. Goddard, and G. R. Kennedy, 1980b: Rain drop sizes and rainfall raᵗe measured by dual-polarization radar. Nature, 285, 195-198.

Hall, M. P. M., S. M. Cherry and J. W. F. Goddard, 1980c: Dual-polarization radar data for evaluation of earth-space radio link attenuation. Proc. AGARD Symposium on Propagation Effects in Space/ Earth Paths London, UK, pp. 8-1 to 8-10.

Harrold, T. W., 1967: The attenuation of 8.6 mm wavelength radiation in rain. Proc. Inst. Elec. Eng. London, 114, 201-203.

Hitschfeld, W., and J. Bordan, 1954: Errors inherent in the radar measurement of rainfall at attenuating wavelengths. J. Meteor., 11, 58-67.

Hogg, D. C., and T. S. Chu, 1975: The role of rain in satellite communications. Proc. IEEE, 63, 1308-1331.

Humphries, R. G., 1974: Observations and calculations of depolarization effects at 3 GHz due to precipitation. J. Rech. Atmos., 8, 155-161.

Humphries, R. G., and B. L. Barge, 1982: Circular polarization for precipitation measurement. To be presented at Multi-Parameter Radar Measurements of Precipitation Symposium, Bournemouth, England, August 1982.

Ippolito, L. J., 1971: Effects of precipitation on 15.3 and 31.6 GHz earth-space transmissions with the ATS-V satellite. Proc. IEEE, 59, 189-205.

Jameson, A. R., and K. V. Beard, 1982: Raindrop axial ratios. J. Appl. Meteor., 21, 257-259.

Jameson, A. R., and A. J. Heymsfield, 1980: Hail growth mechanisms in Colorado Storm. Part I: dual-wavelength radar observations. J. Atmos. Sci., 37, 1763-1778.

Jones, D. M. A., 1956: Rainfall drop-size distribution and radar reflectivity. Res. Rept. 6, Illinois State Water Survey, Meteor. Lab., Urbana, IL 20 pp.

Joss, J., and A. Waldvogel, 1970: A method to improve the accuracy of radar measured amounts or precipitation. Preprints 14th AMS Conf. on Radar Meteorology, Amer. Meteor. Soc., Boston, pp. 237-238.

Joss, J., J. C. Thams, and A. Waldvogel, 1968: The variation of rain drop size distribution in Locarno. Proc. Int. Conf. on Cloud Physics, Toronto, Ontario, Canada, Aug. 26-30.

Joss, J., R. Cavalli, and R. K. Crane, 1974: Good agreement between theory and experiment for attenuation data. J. Rech. Atmos., 8, 299-318.

Kaul, R., R. Wallace, and G. Kinal, 1980: A Propagation Effects Handbook for Satellite Systems Design, NASA Communications Division, Tech. Rep. ORI TR 1679.

Knollenberg, R. G., 1976: Three new instruments for cloud physics measurements. Preprints International Conf. on Cloud Physics, Amer. Meteor. Soc., Boston, pp. 554-561.

Kostarev, V. V., and A. A. Chernikov, 1968: The adjustment of radar estimates of rainfall with radar attenuation data. Preprints 13th AMS Conf. on Radar Meteorology, Amer. Meteor. Soc., Boston, pp. 396-399.

Krehbiel, P. R., and M. Brook, 1979: A broad-band noise technique for fast scanning radar observations of clouds and clutter targets. IEEE Trans. Geosci. Electron., GE-17, 196-204.

Laws, J. O., and D. A. Parsons, 1943: The relation of raindrop-size to intensity. Trans. Amer. Geophys. Union, 24, 452-460.

Lu, Da-ren, 1978: Preliminary investigation of areal precipitation by a ground-based microwave radiometer. Proc. 12th Int. Symp. on Remote Sensing of Environ., April 20-26, 1978, Manila, Phillippines, pp. 523-534.

Lu, Da-ren, and Lin Hai, 1980: Comparisons of radar and microwave radiometer in precipitation measurements and their combined use. Acta Atmospherica Sinics, 1980, No. 1 (in Chinese).

Marshall, J. S., and W. M. K. Palmer, 1948: The distribution of rain-drops with size. J. Meteor., 5, 165-166.

Marshall, J. S., R. C. Langille, and W. M. K. Palmer, 1947: Measurement of rainfall by radar. J. Meteor., 4, 165-166.

Masuko, H., K. Okamoto, S. Yoshikado, H. Inomata, T. Ojima, M. Fujita, and N. Fugono, 1981: Application of the airborne microwave rain-scatterometer/radiometer system to the remote sensing of rains and wind vector measurements over the ocean. To be published in Proc. of the 7th Canadian Symp. on Remote Sensing (Winnipeg, Sept. 8-11).

McCormick, K. S., 1972: A comparison of precipitation attenuation and radar backscatter along earth-space paths. IEEE Trans. Antennas Propagat., AP-20, 747-755.

Medhurst, R. G., 1965: Rainfall attenuation of centimeter waves: Comparison of theory and experiment. IEEE Trans. Antennas Propag., AP-13, 550-563.

Meneghini, R., J. Eckerman, and D. Atlas, 1982: Determination of rain rate from a spaceborne radar using measurements of total attenuation. (Accepted for publication in IEEE Trans. Geosci. and Remote Sening.)

Mueller, E, 1965: Radar Rainfall Studies. Ph.D. Dissertation. University of Illinois.

Newell, R. E., S. G. Geotis, A. Fleisher, 1957: The shape of rain and snow at microwave lengths. MIT Weather Radar Research Report., No. 28, 103 p.

Norbury, J. R., and W. J. K. White, 1972: Microwave attenuation at 35.8 GHz due to rainfall. Electron. Lett., 8, 91-92.

Oguchi, T., 1981: Scattering from hydrometeors: A survey. Radio Science, 16, 691-730.

Olsen, R. L., 1981: Cross polarization during precipitation on terrestrial links. A review. Radio Science, 16, 761-780.

Penzias, A. A., 1970: First result from 15.3 GHz earth-space propagation study. Bell Sys. Tech. J., 49, 1242-1244.

Pruppacher, H. R., and K. V. Beard, 1970: A wind tunnel investigation of the internal circulation and shape of water drops falling at terminal velocity in air. Quart. J. Royal Meteor. Soc., 96, 247-256.

Ryde, J. W., 1941: Echo intensities and attenuation due to clouds, rain, hail, sand and dust storms. Rept. No 7831, General Electric Co., Wembley, England.

Ryde, J. W., 1946: The attenuation and radar echos produced at centimeter wavelengths by various meteorological phenomena. Meteorological Factors in Radio Wave Propagation, pp. 169-188. London: Physical Society.

Seliga, T. A., and V. N. Bringi, 1976: Potential use of radar differential reflectivity measurements at orthogonal polarizations for measuring precipitation. J. Appl. Meteor., 15, 69-76.

Seliga, T. A., and V. N. Bringi, 1977: Scattering from non-spherical hydrometeors. Proc. URSI Open Symposium, Comm. F, La Baule, France. pp. 199-204.

Seliga, T. A., and V. N. Bringi, 1978: Differential reflectivity and differential phase shift: Applications in radar meteorology. Radio Science, 13, 271-275.

Seliga, T. A., V. N. Bringi, and E. A. Mueller, 1980: Comparison of rainfall rates derived from differential reflectivity and disdrometer measurements. Preprints 19th AMS Conf. on Radar Meteorology, Amer. Meteor. Soc., Boston, pp. 523-525.

Seliga, T. A., V. N. Bringi, and H. H. Al-Khatib, 1981: A preliminary study of comparative measurement of rainfall rate using the differential reflectivity radar technique and a raingage network. J. Appl. Meteor., 20, 1362-1368.

Semplak, R. A., and R. H. Turrin, 1969: Some measurements of attenuation by rainfall at 18.5 GHz. Bell Sys. Tech. J., 48, 1767-1788.

Srivastava, R. C., and R. E. Carbone, 1971: The effect of signal fluctuations on the performance of dual-wavelength radar hail detector. Tech. Rept. #20, Lab. for Atmos. Probing, University of Chicago, Chicago, Illinois.

Srivastava, R. C., and A. R. Jameson, 1977: Radar detection of hail. Meteor. Monogr., No. 38, 269-277.

Stickel, P. G. and T. A. Seliga, 1981: Cloud liquid water content comparisons in rain using radar differential reflectivity measurements and aircraft measurements. Preprints 20th AMS Conf. on Radar Meteorology, Amer. Meteor. Soc., Boston, pp. 567-571.

Stogryn, A., 1975: Error analysis of the Goldhirsh-Katz method of rainfall determination by the use of a two frequency radar. Rpt. No. 1833TR-4, Aerojet Electrosystems Co., Azusa, CA.

Strickland, J. I., 1974: The measurement of slant path attenuation using radar, radiometers, and satellite beacons. J. Rech. Atmos., 8, 347-358.

Sulakvelidze, G. K., and Y. A. Dadali, 1968: The measurement of precipitation intensity with a multi-wavelength radar. Proc. Third All-Union Conf. Radar Meteor., Hydrometeor. Service, Moscow, pp. 31-42.

Twomey, S., 1953: On the measurement of precipitation intensity by radar. J. Meteorol., 10, 66-67.

Ulbrich, C. W., 1981: Potential of dual measurement techniques for accurate determination of instantaneous rainfall rate from space. Precipitation Measurements from Space. Workshop Report, Oct. 1981, NASA Goddard Space Flight Center, Greenbelt, MD, pp. D238-287.

Ulbrich, C. W., and D. Atlas, 1975: The use of radar reflectivity and microwave attenuation to obtain improved measurement of precipitation. Preprints 16th AMS Conf. on Radar Meteorology, Amer. Meteor. Soc., Boston, pp. 496-503.

Ulbrich, C. W., and D. Atlas, 1977: A method for measuring precipitation parameters using radar reflectivity and optical extinction. Ann. d. Telecomm., 32, 415-421.

Ulbrich, C. W., and D. Atlas, 1978: The rain parameter diagram: methods and applications. J. Geophys.Res., 83, 1319-1325.

Ulbrich, C. W., and D. Atlas, 1982a: Assessment of the contribution of differential polarization to improved rainfall measurements. To be presented at Multi-Parameter Radar Measurements of Precipitation Symposium, Bournemouth, England, August 1982.

Ulbrich, C. W., and D. Atlas, 1982b: Hail parameter relations: A comprehensive survey. J. Appl. Meteor., 21, 22-43.

Waldvogel, A. 1974: The N_0 jump of raindrop spectra. J. Atmos. Sci., 31, 1067-1078.

Wang, T., K. B. Earnshaw, and R. S. Lawrence, 1979: Path-averaged measurements of rain rate and raindrop size distribution using a fast-response optical sensor. J. Appl. Meteor., 18, 654-660.

Wexler, R., 1976: K-band attenuation by rain at constant reflectivity. Preprints 17th AMS Conf. on Radar Meteorology, Amer. Meteor. Soc., Boston, pp. 72-74.

Wexler, R., and D. Swingle, 1947: Radar storm detection, Bull. Amer. Meteor. Soc., 28, 159-167.

Wilson, J. W., and E. A. Brandes, 1979: Radar measurement of rainfall-- A summary. Bull. Amer. Meteor. Soc., 60, 1048-1058.

Wilson, R. W., and A. A. Penzias, 1966: Effect of precipitation on transmission through the atmosphere at 10 microns. Nature, 211, 1081.

Yamada, M., A. Ogawa, O. Furuta, and H. Yokoi, 1978: Measurement of rain attenuation by dual-frequency radar. Summaries of Papers, Inter. Symp. on Ant. and Propaga., ISAP, Japan, pp. 469-472.

Zavody, A. M., 1974: Effect of scattering by rain on radiometric measurements at millimeter wavelengths. Proc. Inst. Elec. Engr., 121, 257-263.

TABLE OF SYMBOLS

Symbol	Units	Definition
A	$(db\ km^{-1})$	microwave attenuation.
$A_i(x)$	$(db\ km^{-1})$	microwave attenuation at wavelength λ_i and distance x.
$A(\lambda)$	$(db\ km^{-1})$	microwave attenuation at wavelength λ.
$\overline{A}$	$(db\ km^{-1})$	path-average microwave attenuation.
a	$(mm^{6-b}\ h^b\ m^{-3})$	coefficient in Z-R relation $R = a_Z^{\ b}$.
a_x	(see Table 1)	coefficient in relation between parameter X, Z and D_o (Table 1).
AAD	(%)	average absolute deviation.
AL	(db)	total path attenuation.
BB		bright band.
b		exponent in Z-R relation $Z = aR^b$.
C	(cm^{2-n})	coefficient in power law approximation to total attenuation cross section $Q_t(D) = CD^n$.
C_i	$(w\ m^5\ mm^{-6})$	radar calibration constant.
C_h	$(w\ m^5\ mm^{-6})$	radar calibration constant for horizontal polarization.
C_v	$(w\ m^5\ mm^{-6})$	radar calibration constant for vertical polarization.
C_m	$(db\ cm^{-1.5})$	coefficient in power law approximation $Z_{DR} = C_m D_o^{1.5}$.
CDR	(db)	circular depolarization ratio.
D	(cm)	equivalent spherical raindrop diameter.
D_o	(cm)	size distribution parameter median volume diameter.
D_{max}	(cm)	upper limit of raindrop diameters in drop size distribution.
D_{min}	(cm)	lower limit of raindrop diameters in drop size distribution.
DSD		drop size distribution.
e_x		exponent in relation between parameter X, Z and D_o (Table 1).
$F_A(D_o,m)$		numerical integral in definition of A (Table 1).

Symbol	Units	Definition
$F_R(D_o, m)$		numerical integral in definition of R (Table 1).
f_j		dimensionless function relating rainfall rate to power return to radar.
G		dimensionless third moment of the raindrop mass distribution $$G = \frac{\int D^6 N(D)\, dD}{D_o^3 \int D^3 N(D)\, dD}.$$
H	(cm^4)	$H = 10^6 \lambda^4 / \pi^5 |K|^2$
h	(km)	range resolution; interval between range gates.
$I(\bar{\Lambda})$		$$I(\bar{\Lambda}) = \int_D \sigma(D) \exp(-\bar{\Lambda}D)\, dD.$$
$|K|^2$		$|K|^2 = 0.93$, refractivity factor for water.
L	(km)	total path length.
L_ν	(km)	path length spanned by ν range gates.
m		exponent in gamma size distribution function $N(D) = N_o D^m \exp(-\Lambda D)$.
$N(D)$	$(m^{-3}\, cm^{-1})$	raindrop size distribution.
$N(D,x)$	$(m^{-3}\, cm^{-1})$	raindrop size distribution at distance x from radar.
N_o	$(m^{-3}\, cm^{-1})$	raindrop size distribution parameter.
$\bar{N}_o$	$(m^{-3}\, cm^{-1})$	path- or interval-average size distribution parameter.
$N_o(x)$	$(m^{-3}\, cm^{-1})$	raindrop size distribution parameter at distance x from radar.
N_{oi}	$(m^{-3}\, cm^{-1})$	raindrop size distribution parameter in ith range gate from radar.
N_T	(m^{-3})	total raindrop number concentration.
n		exponent in power law approximation to total attenuation cross section $Q_t(D) = CD^n$.
$P(\lambda_i, r_j)$	(watts)	power returned to radar at wavelength λ_i from range r_j.
$P_h(r_j)$	(watts)	power return to radar from range r_j at horizontal polarization.
$P_v(r_j)$	(watts)	power return to radar from range r_j at vertical polarization.
$\langle P_h \rangle$	(watts)	average power return to radar at horizontal polarization.

Symbol	Units	Definition
$\langle P_v \rangle$	(watts)	average power return to radar at vertical polarization.
$Q_t(D)$	(cm^2)	total attenuation cross section of raindrop of diameter D.
$Q_t(D,\lambda)$	(cm^2)	total attenuation cross section of raindrop of diameter D at wavelength λ.
R	(mm h^{-1})	rainfall rate.
R_i	(mm h^{-1})	rainfall rate at ith range gate from radar.
$\overline{R}$	(mm h^{-1})	path average rainfall rate.
R_{actual}	(mm h^{-1})	rainfall rate found from raindrop size spectrum data.
R_{calc}	(mm h^{-1})	rainfall rate found from empirical relation or from multiple-measurement simulation.
r_j	(m)	radar range.
T_a	(K)	physical absorber temperature.
T_b	(K)	microwave brightness temperature.
T_i	(watts km^2)	$T_i = P(\lambda_i, r_k) r_k^2$
$v(D)$	(m s^{-1})	raindrop fallspeed in still air.
W	(g m^{-3})	liquid water content.
$\overline{W}$	(g m^{-3})	path-average liquid water content.
X	(see Table 1)	any of the parameters W, R, Σ, A, N_T, N_0 (Table 1).
x	(cm, km)	distance.
Z	($mm^6\ m^{-3}$)	radar reflectivity factor.
$Z(\lambda_i, r_j)$	($mm^6\ m^{-3}$)	radar reflectivity factor at wavelength λ_i and at range r from radar.
Z_{DR}	(db)	differential radar reflectivity factor.
$\langle Z_{DR} \rangle$	(db)	pulse-average differential reflectivity factor.
α_m		$(\Lambda D_0)_m = 3.67 + m$.
β		exponent in A-Z relation $A = \xi Z^\beta$.
β_m		$\beta_m = \alpha_m^3 / \Gamma(7 + m)$.
r_p		power ratio $\dfrac{P(\lambda_1,r_j)\ P(\lambda_2,r_k)}{P(\lambda_1,r_k)\ P(\lambda_2,r_j)}$.

Symbol	Units	Definition
$\Gamma(a)$		complete gamma function $$\Gamma(a) = \int_0^\infty u^{a-1} e^{-u} \, du \ .$$
γ	(m s^{-1} cm$^{-0.67}$)	coefficient in power law approximation to drop fallspeed $v(D) = \gamma \, D^{0.67}$ $\gamma = 17.67$ m s^{-1} cm$^{-0.67}$.
ϵ_{ij}		$\epsilon_{ij} = 1 \quad i \neq j$ $\epsilon_{ij} = 0.5 \quad i = j$.
η_a	(cm^2 m^{-3})	radar reflectivity above bright band.
η_b	(cm^2 m^{-3})	radar reflectivity below bright band.
η_p	(cm^2 m^{-3})	peak radar reflectivity in bright band.
Λ	(cm^{-1})	raindrop size distribution parameter.
$\overline{\Lambda}$	(cm^{-1})	path- or interval-average size distribution parameter.
λ, λ_i	(cm)	wavelength.
$\mu_X(D_o, m)$		dimensionless pseudomoment of the drop size distribution for parameter X. (Table 1).
ν		total number of range gates.
ξ	(db mm$^{-6\beta}$ m$^{3\beta}$)	coefficient in A-Z relation $A = \xi \, Z^\beta$.
Σ	(km^{-1})	optical extinction.
σ	(cm^{-1})	absorber attenuation coefficient.
$\sigma(D)$	(cm^2)	radar backscattering cross section of a raindrop of diameter D.
$\sigma_h(D)$	(cm^2)	radar backscattering cross section at horizontal polarization for a raindrop with equivalent diameter D.
$\sigma_v(D)$	(cm^2)	radar backscattering cross section at vertical polarization for a raindrop with equivalent diameter D.

Table I

Parameter X, coefficient a_x, exponent e_x, and pseudomoment $\mu_x(D_o, m)$ in

$$X = a_x\, \mu_x(D_o, m)\, Z\, D_o^{-e_x}$$

in terms of reflectivity factor $Z(mm^6\ m^{-3})$ and median volume diameter D_o(cm).

X	a_x	e_x	$\mu_x(D_o, m)$
$W(g\ m^{-3})$	$\frac{\pi}{6} \times 10^{-6}\ g\ cm^3\ mm^{-6}$	3	$\beta_m\, \Gamma(4+m)$
$R(mm\ h^{-1})$	$0.6\pi\ \gamma \times 10^{-6}\ cm^{2.33}\ m^3\ mm^{-5}\ h^{-1}$	2.33	$\alpha_m^{4+m}\, \beta_m F_R(D_o,m) \qquad [\alpha_m^{2.33}\, \beta_m \Gamma(4.67+m)]$
$\Sigma(km^{-1})$	$0.5\pi \times 10^{-7}\ cm^4\ m^3\ mm^{-6}\ km^{-1}$	4	$\alpha_m \beta_m \Gamma(3+m)$
$A(db\ km^{-1})$	$4.34 \times 10^{-7}\ C\ db\ m^3\ cm^{6-n}\ mm^{-6}\ km^{-1}$	6-n	$\alpha_m^{4+m}\, \beta_m F_A(D_o,m) \qquad [\alpha_m^{6-n}\, \beta_m \Gamma(n+m+1)]$
$N_T(m^{-3})$	$10^{-6}\ cm^6\ mm^{-6}$	6	$\alpha_m^3\, \beta_m \Gamma(1+m)$
$N_o(m^{-3})$	$10^{-6}\ cm^{6+m}\ mm^{-6}$	7 + m	$\alpha_m^{4+m}\beta_m$

$$\alpha_m = (\Lambda D_o)_m = 3.67 + m \qquad F_R(D_o,m) = \gamma^{-1} D_o^{-(m+4.67)} \qquad \int_0^\infty v(D)\, D^{3+m}\, e^{-\Lambda D}\, dD$$

$$\beta_m = \frac{\alpha_m^3}{\Gamma(7+m)} \qquad F_A(D_o,m) = C^{-1} D_o^{-(m+n+1)} \qquad \int_0^\infty Q_t(D)\, D^m\, e^{-\Lambda D}\, dD$$

PRECEDING PAGE BLANK NOT FILMED

FIGURES

Fig. 1a: Rain parameter diagram: base diagram. Radar reflectivity
            factor versus rainfall rate with isopleths of median volume
            diameter D_0, size distribution parameter N_0, liquid water
            content W, and optical extinction Σ shown as heavy solid lines,
            light solid lines, heavy dashed curves, and light dashed curves,
            respectively. Also shown as an inset is the differential
            reflectivity factor Z_{DR} as a function of D_0. [from Ulbrich
            and Atlas (1978)].
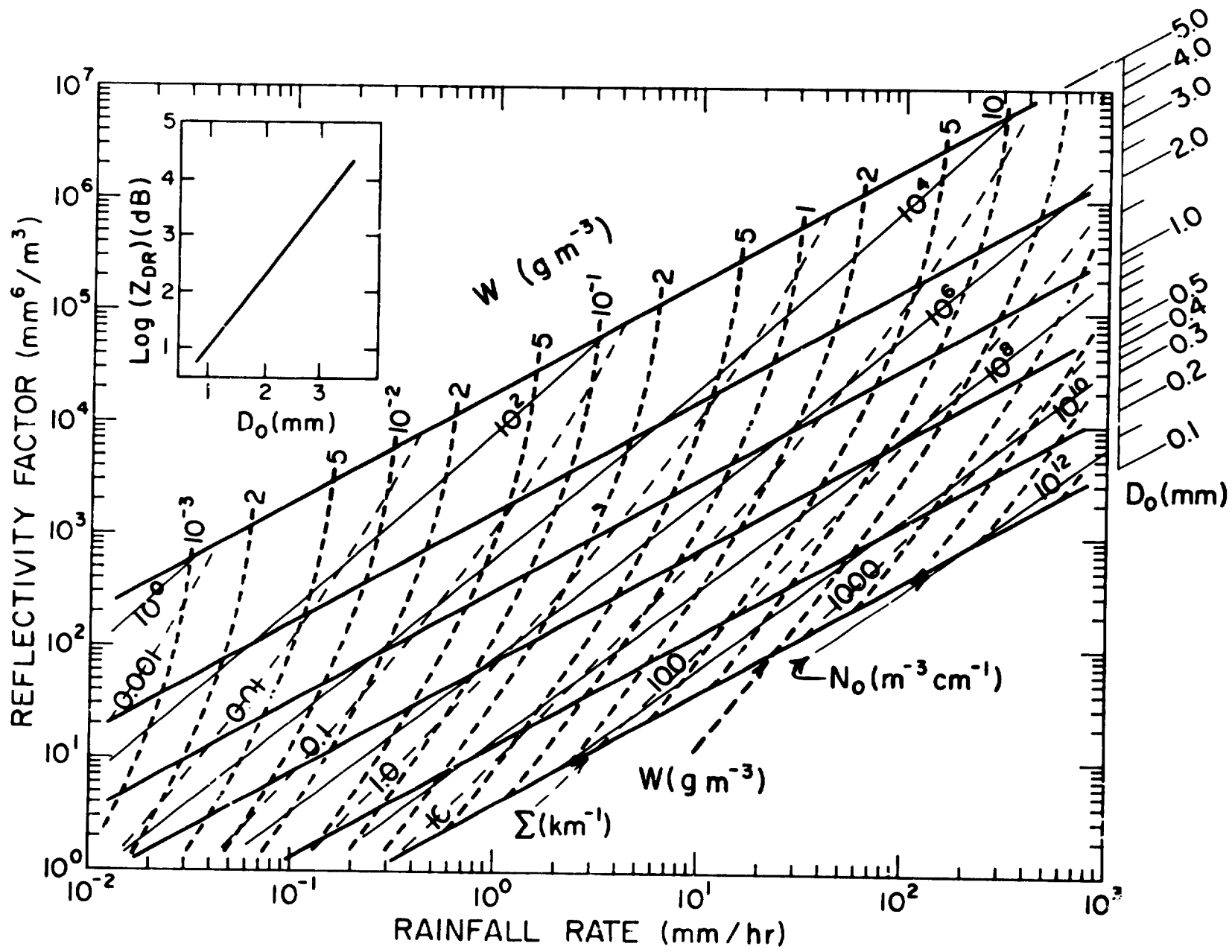
Fig. 1b: Rain parameter diagram: attenuation overlay for λ = 3.22 cm.
Isopleths of microwave attenuation A(db km^{-1}) for temperatures
T = -10, 0, 10 and 20°C are shown as dashed, light solid, dotted
and heavy solid curves, respectively. [from Ulbrich and Atlas
(1978)].

RAINFALL RATE (mm/hr)

REFLECTIVITY FACTOR (mm⁶/m³)

A (db km⁻¹) – 3.22 cm

20°C
10°C
0°C
-10°C

Fig. 1c: Five typical empirical Z-R relations plotted on a simplified
version of the base diagram in Fig. 1a. Also shown as a shaded
area is the part of the diagram within which fall all of the 69
empirical Z-R relations listed by Battan (1973) [after Ulbrich
and Atlas (1978)].

Legend on plot:

MARSHALL-PALMER (1948), $Z = 200\,R^{1.6}$
JOSS-WALDVOGEL (1970), $Z = 300\,R^{1.5}$
JONES (1956), $Z = 486\,R^{1.37}$
BLANCHARD (1953), $Z = 31\,R^{1.71}$
FOOTE (1966), $Z = 520\,R^{1.81}$

Y-axis: REFLECTIVITY FACTOR (mm^6/m^3)

X-axis: RAINFALL RATE (mm/hr)

Right axis label: D_0(mm)

Contour labels: $N_T = 100\ m^{-3}$, $N_T = 10^2\ m^{-3}$, 10^4, 10^6, 10^8
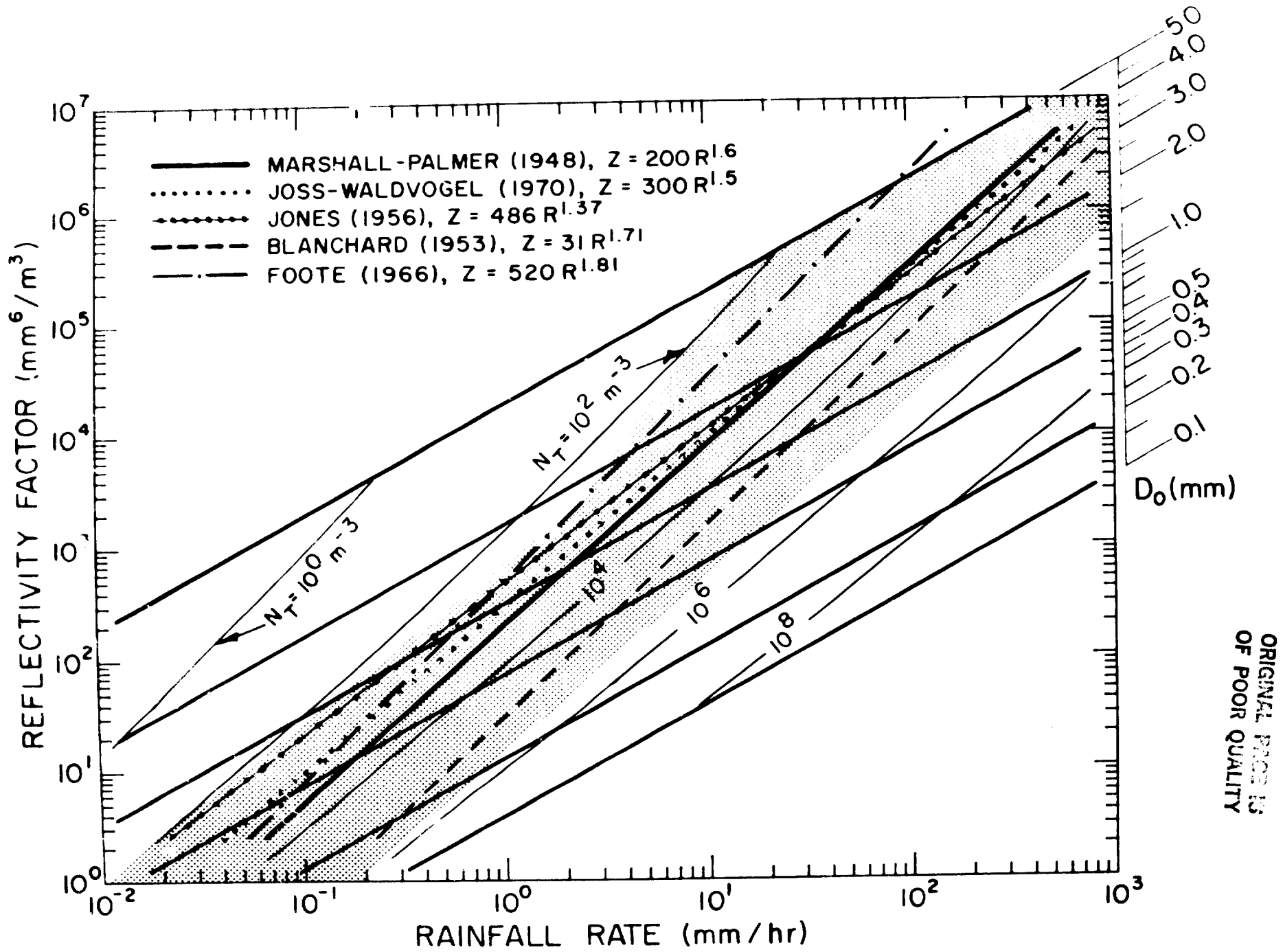
Fig. 2: Coefficient C (db $cm^{-1.5}$) in $Z_{DR} - D_0$ power law approximation, dimensionless third moment of the mass distribution G, and ratios of the pseudomements $\mu_x(m)/\mu_x(0)$ for $X = R$, W, Σ, N_T, N_0 and A versus of the exponent m in the gamma drop size distribution. Each of the curves is labeled with the function to which it corresponds.
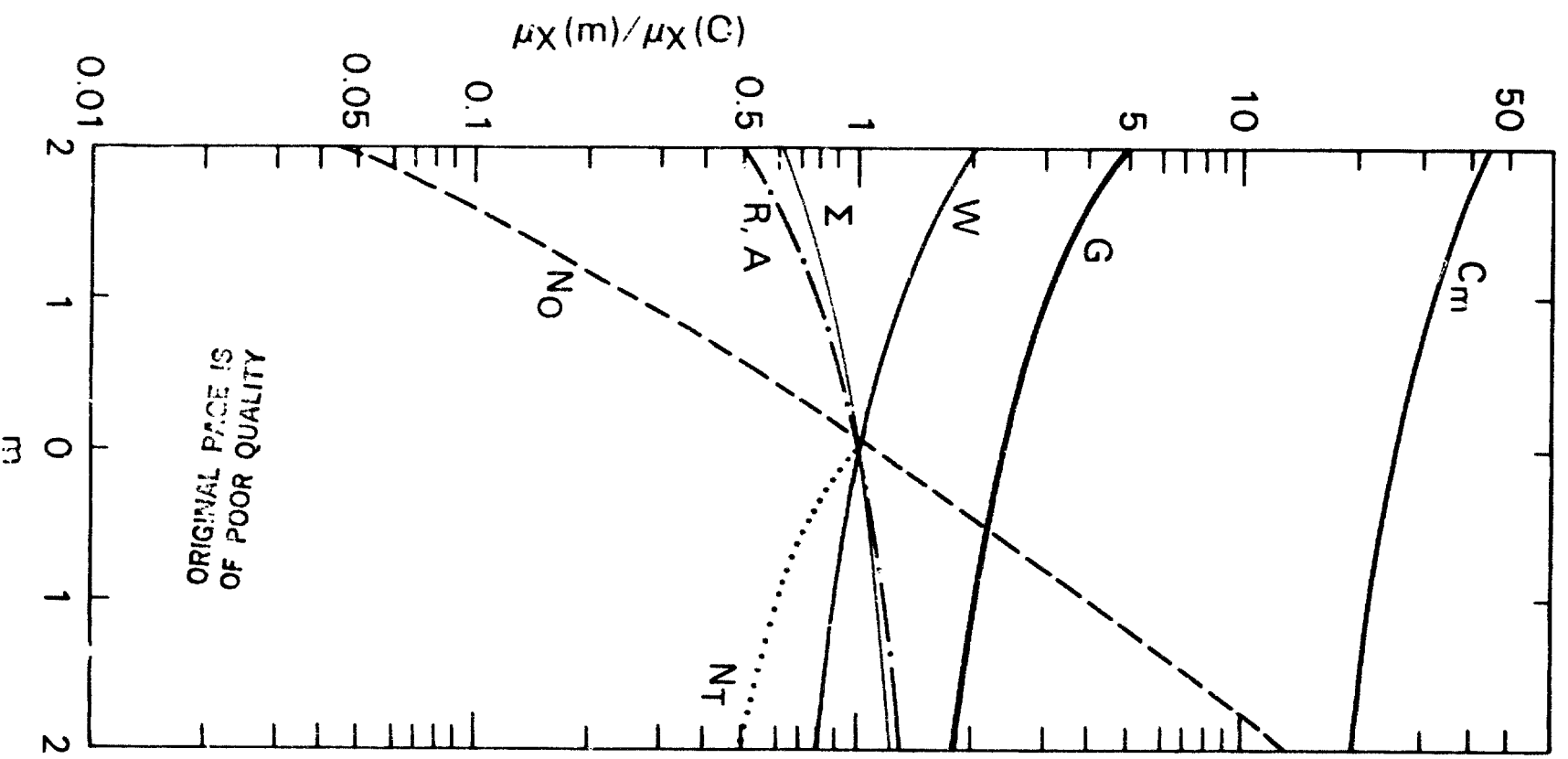
Fig. 3: Comparisons of calculated rainfall rate R_{calc} with actual rainfall rate R_{actual} for single-measurement simulations using a set of drop size spectra described by Ulbrich and Atlas (1977). The upper, center and lower sets of data points correspond to R_{calc} calculated from empirical Z-R, Σ-R relations, respectively, in each of which the remote measurable (Z, Σ or A) was found from the size spectra data. In all cases R_{actual} is determined directly from the size spectra.
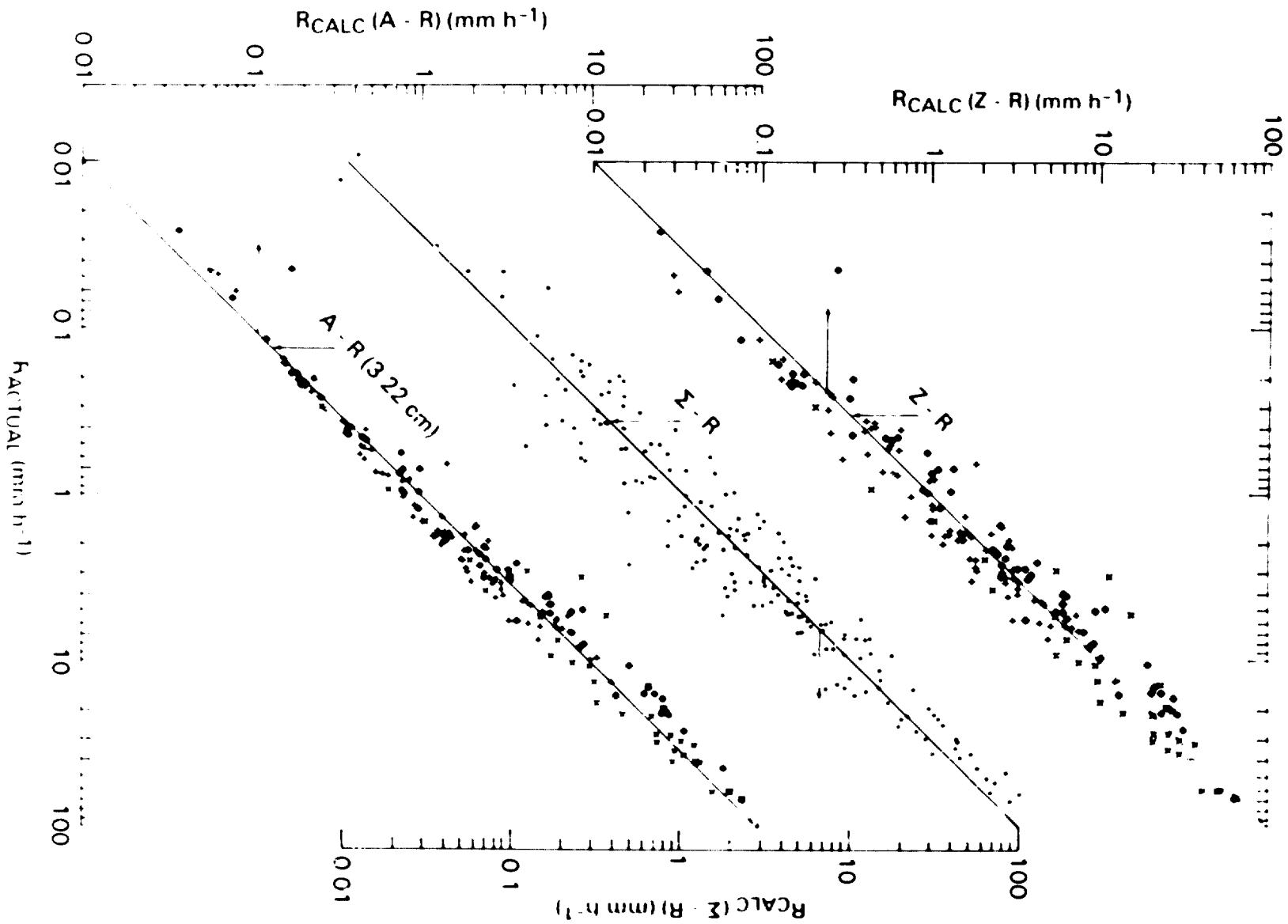
Fig. 4: Comparisons of calculated rainfall rate R_{calc} with actual
rainfall rate R_{actual} for dual-measurement simulations using
the same set of drop size spectra as in Fig. 3. The upper,
second, third and lower sets of data points correspond to R_{calc}
calculated from simulated measurable pairs [Z, A(λ = 1.25 cm)],
[Z, A(λ = 3.22 cm)], [Z, Σ] and [Z, Z_{DR}], respectively, for
which all remote measurables were found from the size spectra
data. In all cases R_{actual} is determined directly from the
size spectra.

C-2
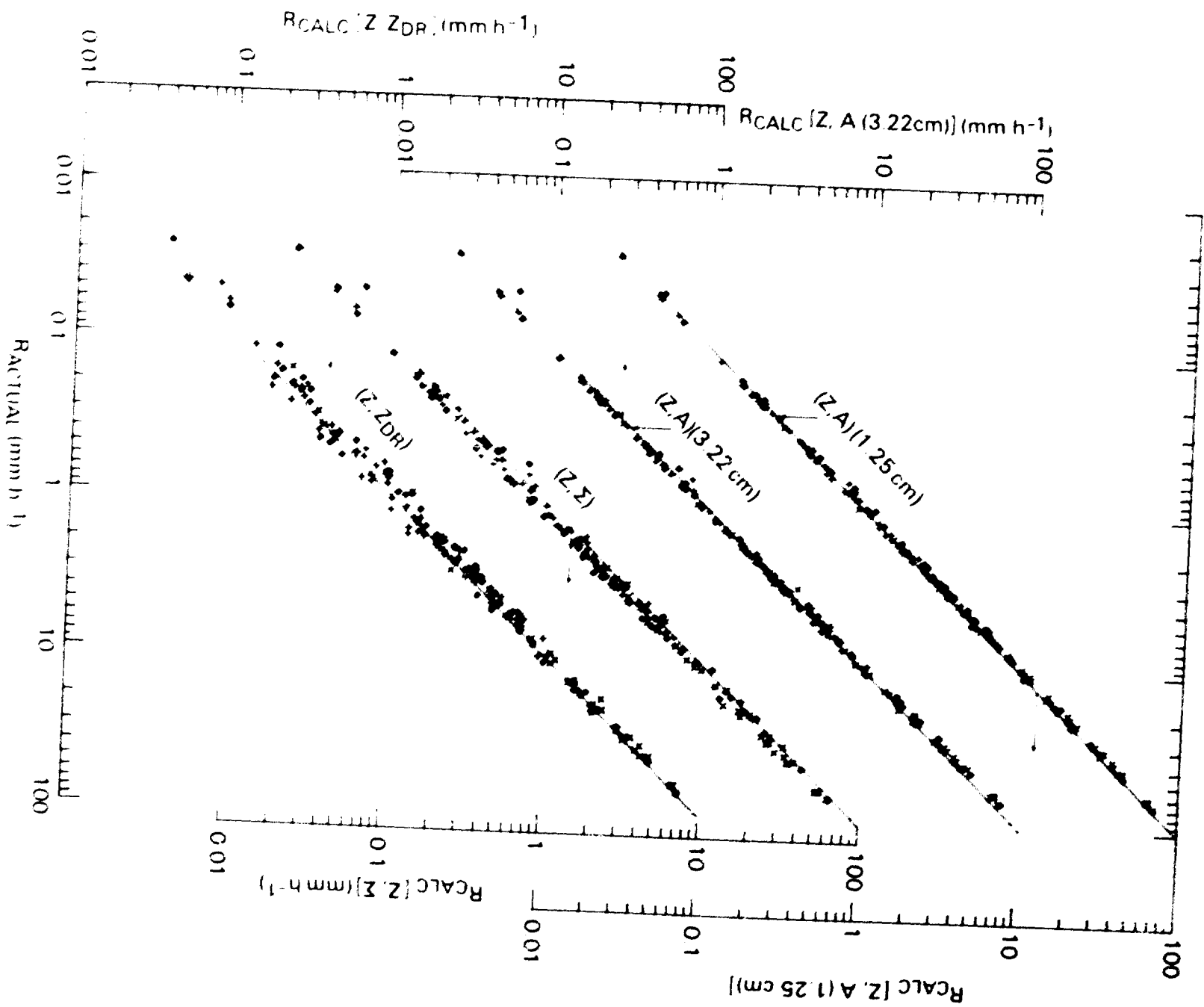
Fig. 5:   Comparison of calculated rainfall rate R_{calc} with actual
rainfall rate R_{actual} for a triple-measurement simulation
using the same set of drop size spectra as in Fig. 3. The
data points correspond to R_{calc} calculated from a simulated
measurable triplet $(Z, Z_{DR}, \Sigma^{calc})$ in which all measurables were
found from the size spectra.
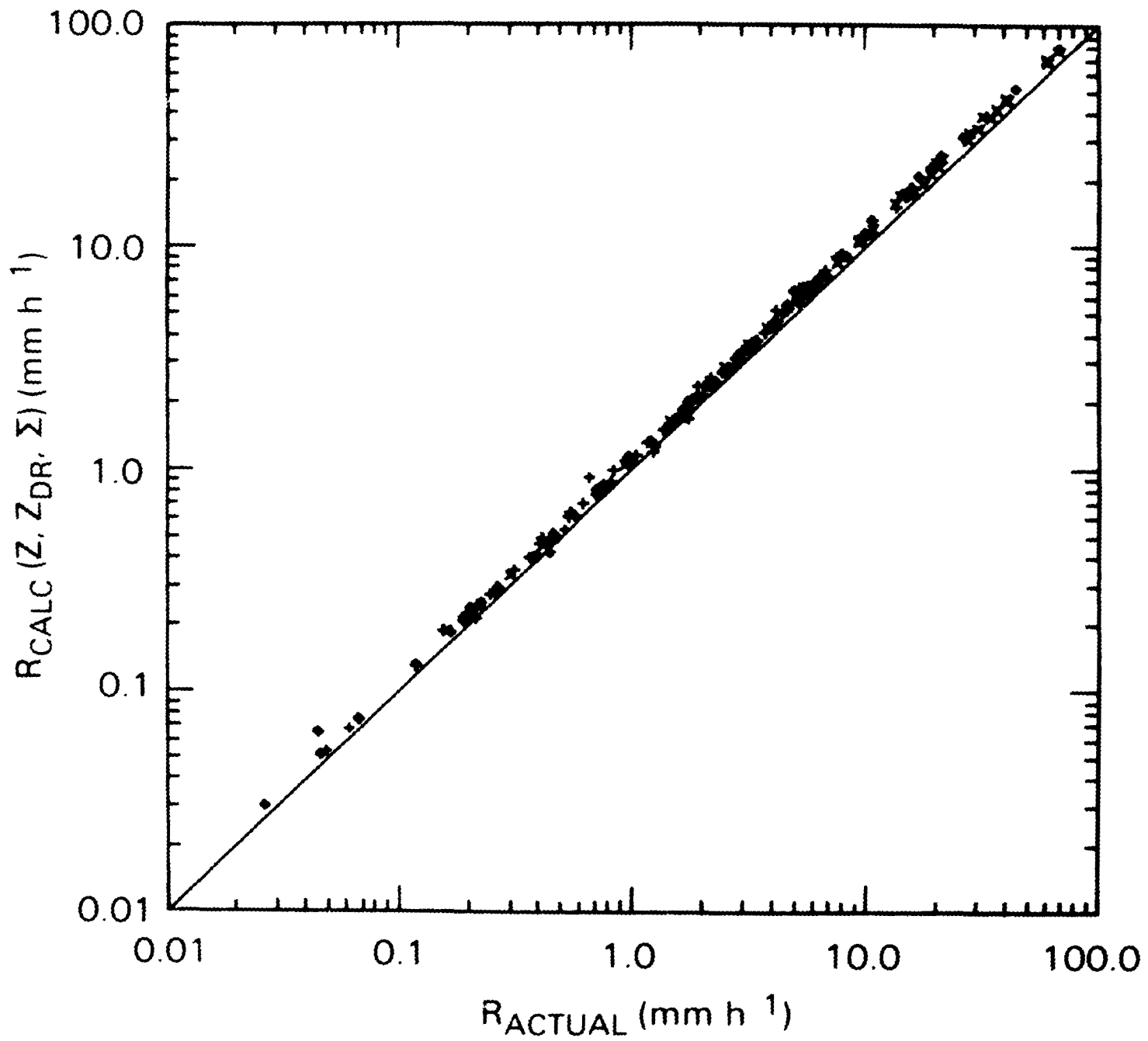
Fig. 6:   Attenuation versus rainfall rate for ten rain showers during
          the summer of 1971 in Slough, England. The crosses are measured
          data points, the solid curve represents a theoretical
          calculation of attenuation as a function of rainfall rate using
          the Laws and Parsons (1943) drop size spectra, and the dashed
          curve is a parabola fitted to the data by least squares [from
          Norbury and White (1972)].
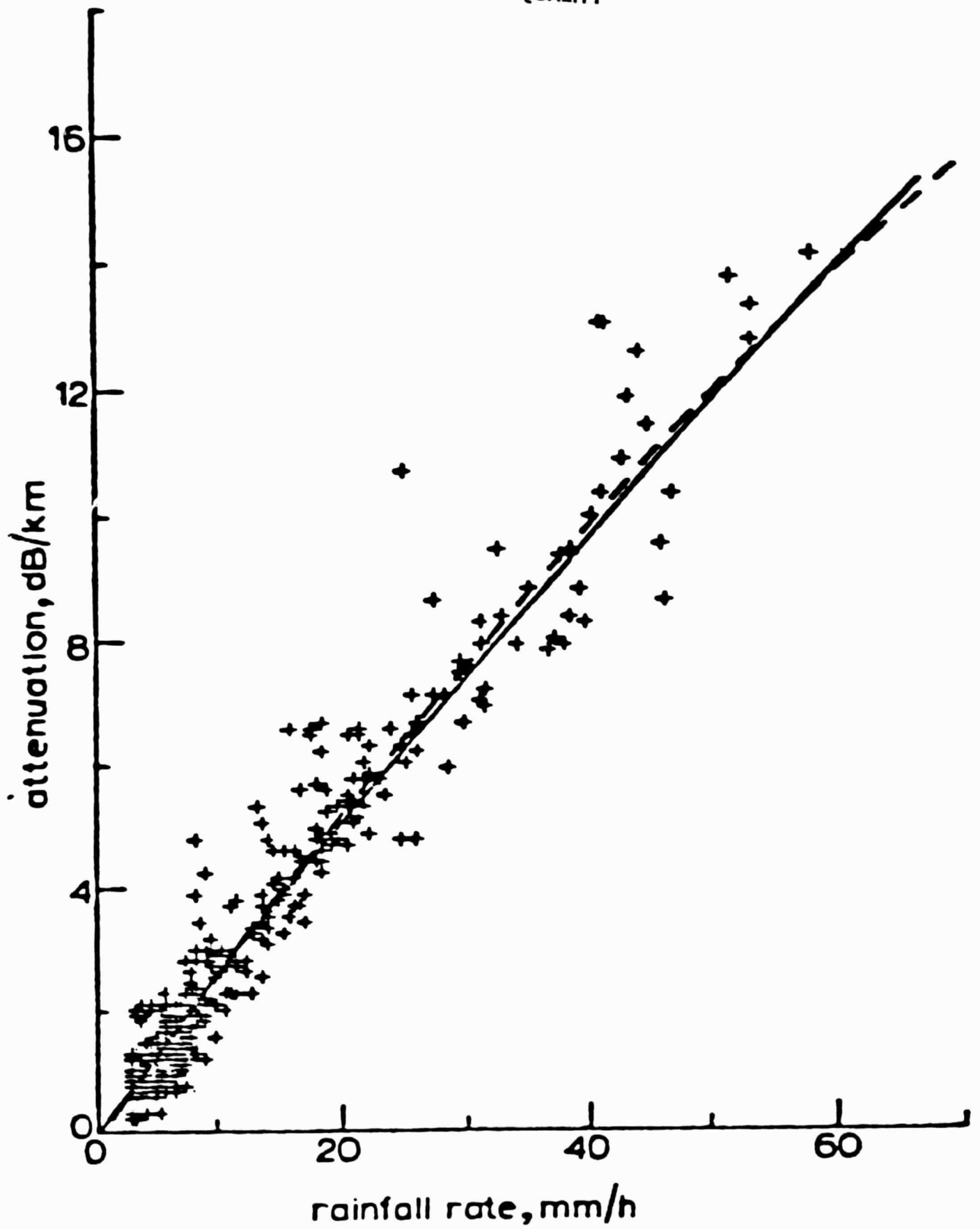
Fig. 7:   Plot of observed total path attenuation γ_{meas} (db) of
microwaves with wavelength equal to 1.62 cm versus path-average
rainfall rate $\langle R \rangle_{av}$ as measured by raingages for 23 rain storms
in New Jersey during the summer of 1967. The circles and
crosses are measured data points, the latter corresponding
to one storm for which there was evidence of an updraft. The
line composed of one long dash and two short dashes is the
theoretical calculation of Gunn and East (1954), the long dash-
short dash line and solid line are power law and linear least
squares fits to the data, respectively, and the upper and lower
dashed lines are the maximum and minimum attenuation-rainfall
rate relations for monodisperse drop size distributions. [from
Semplak and Turrin (1969)].

$\gamma = 0.055 \langle R \rangle_{av}^{1.09}$ dB/km
(GUNN & EAST)

$\gamma = 0.041 \langle R \rangle_{av}^{1.04}$ dB/km

$\gamma = 0.048 \langle R \rangle_{av}$ dB/km
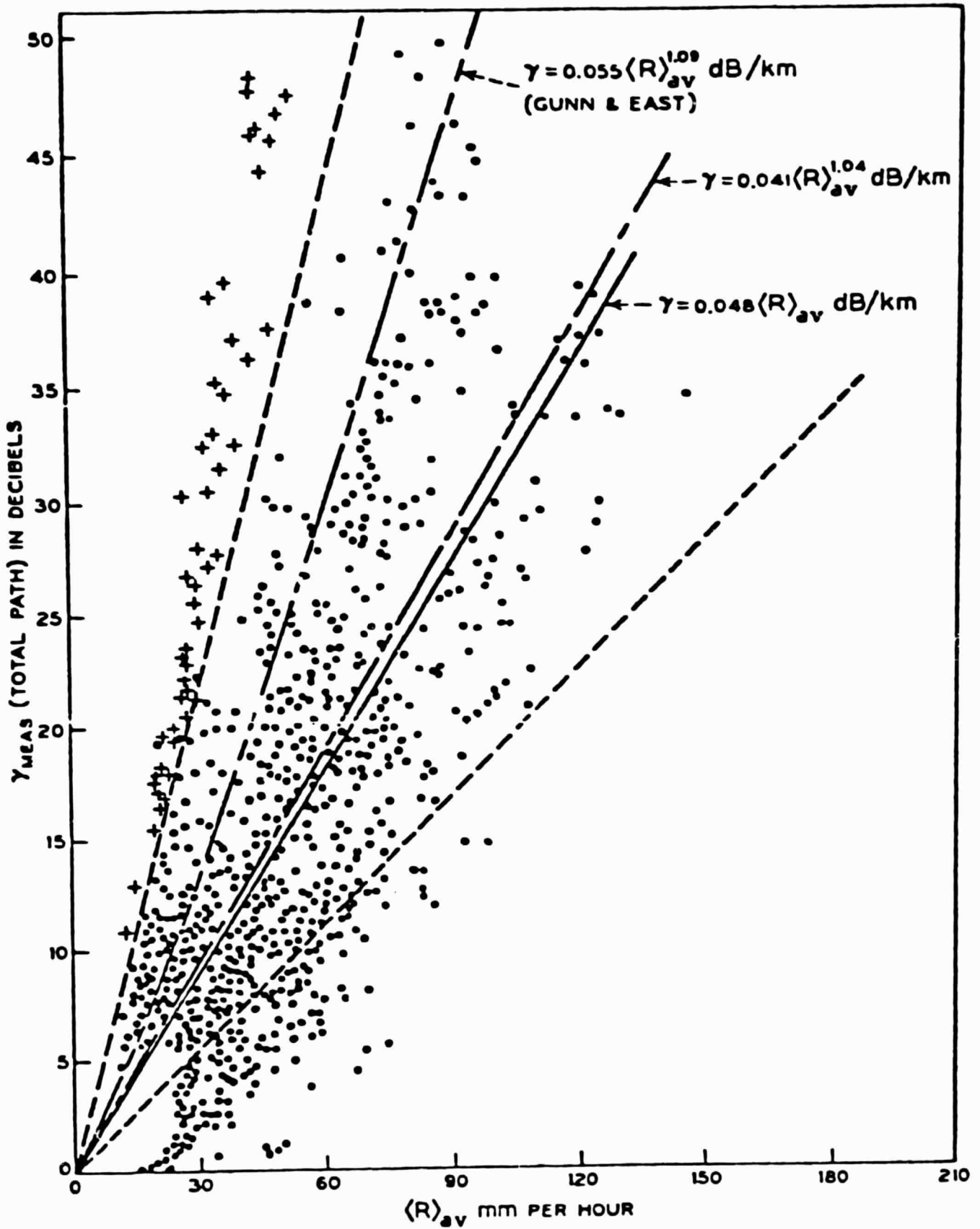
Fig. 8:   Total attenuation measured by a 16 GHz passive radiometer versus attenuation of the 15.3 GHz ATS-5 satellite beacon for a rain shower in New Jersey. The data points are measured values and the dashed line has a slope of 1.1 to account for the difference in frequency of the two signals. [after Penzias (1970)].

16 GHz RADIOMETER ATTENUATION, dB

15.3 GHz SATELLITE SIGNAL ATTENUATION, dB
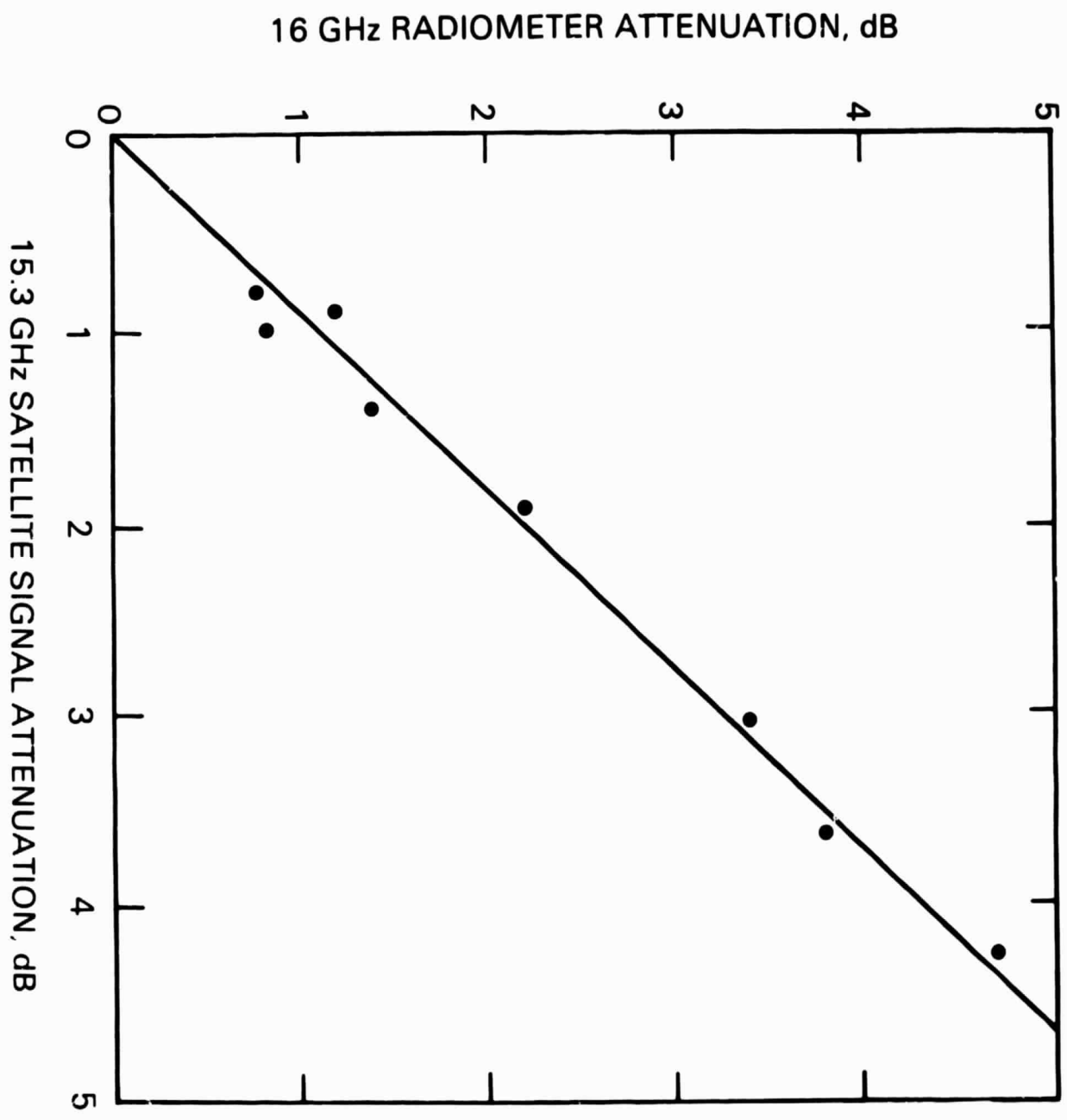
Fig. 9:   Theoretical curves of microwave brightness temperature T_b(k) for a wavelength of 3.2 cm versus path-average rainfall rate R(mm h^{-1}) and total path length L(km). Elevation angle of the radiometer is assumed to be 4°. [after Lu (1978)]
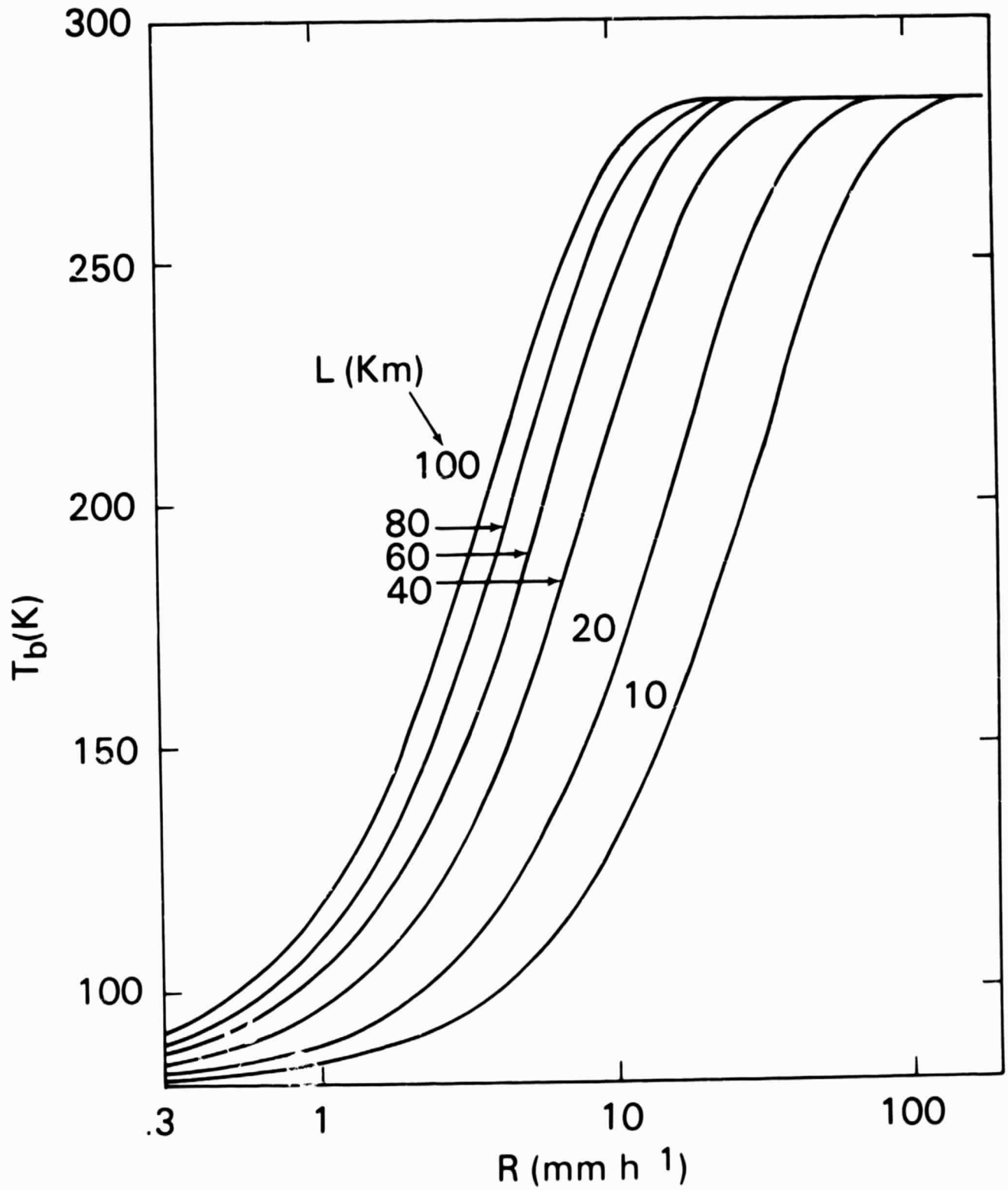
Fig. 10:   Comparison of attenuation at 15.3 GHz calculated from
           radiometric measurements of sky noise temperature with that
           measured directly using the ATS-5 satellite beacon. The solid
           circles represent measured values for a storm in Ottawa, Canada.
           The straight line of unit slope assumes an effective absorber
           temperature of 278K and solid curves above and below that line
           correspond to absorber temperatures of 268K and 288K,
           respectively. [after Strickland (1974)].
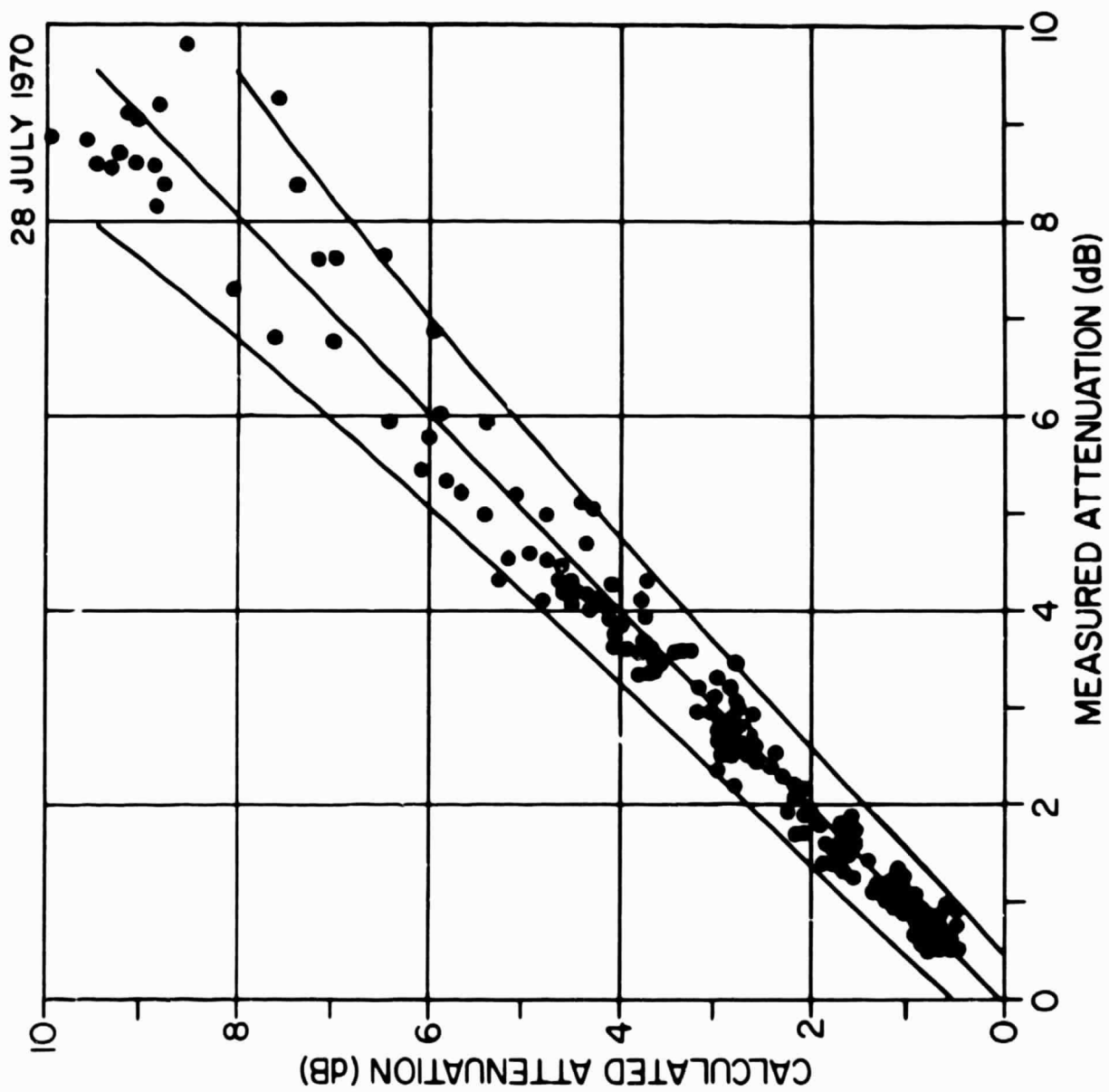
Fig. 11:   (a) Contours of reflectivity factor Z for a thunderstorm
observed by a 2.9 GHz radar scanning in azimuth at an elevation
angle of $\sim$ 6.5°. Also shown along the periphery is the total
attenuation measured using an aircraft beacon at 15 GHz circum-
navigating the storm.
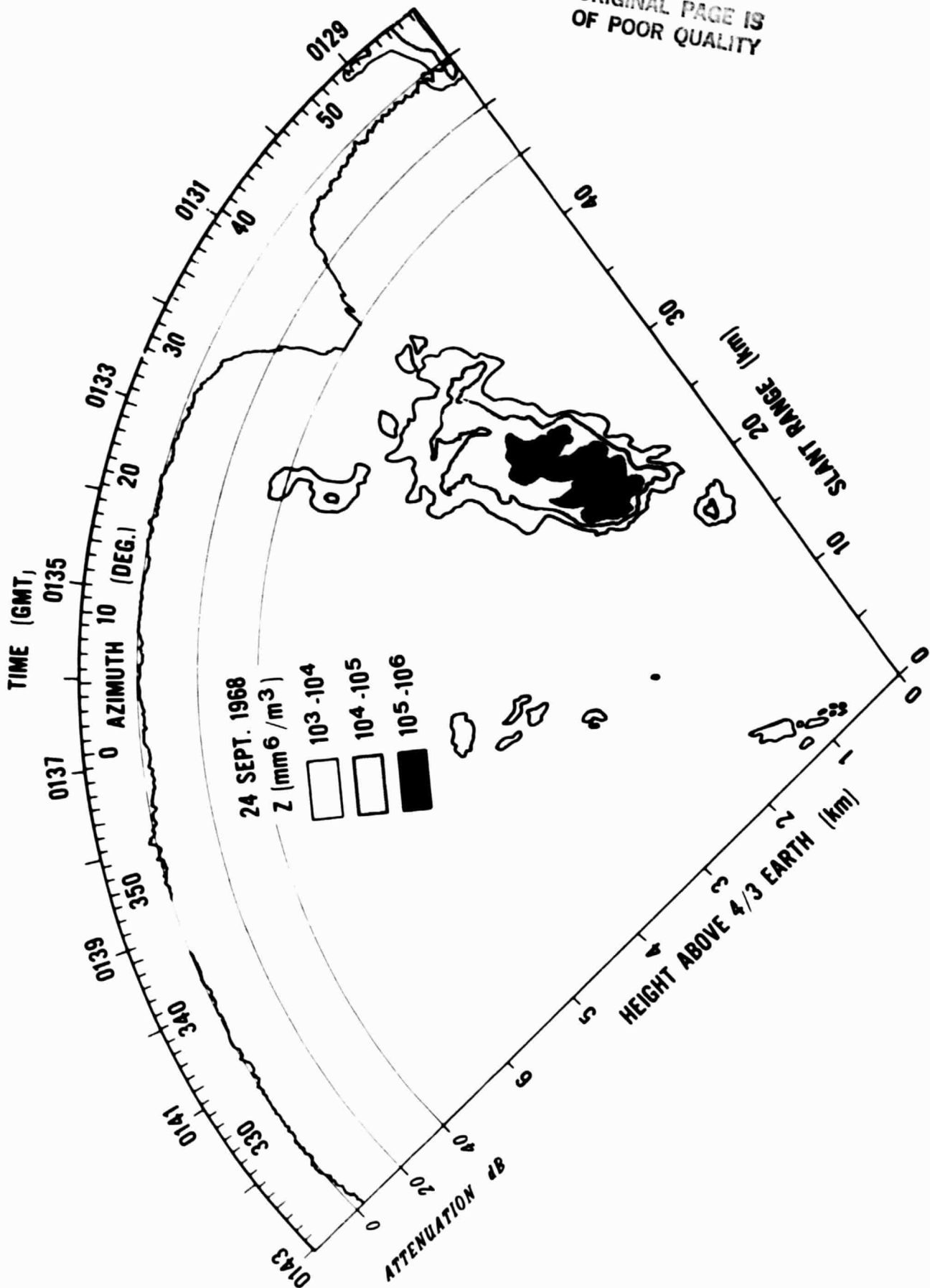
Fig. 11:   (b) Comparison of attenuations measured directly (heavy curves)
            at 4, 8, and 15 GHz using aircraft beacons as in part (a) with
            that computed from the radar data (light curves). [after
            McCormick (1972)].

24 SEPT. 1968
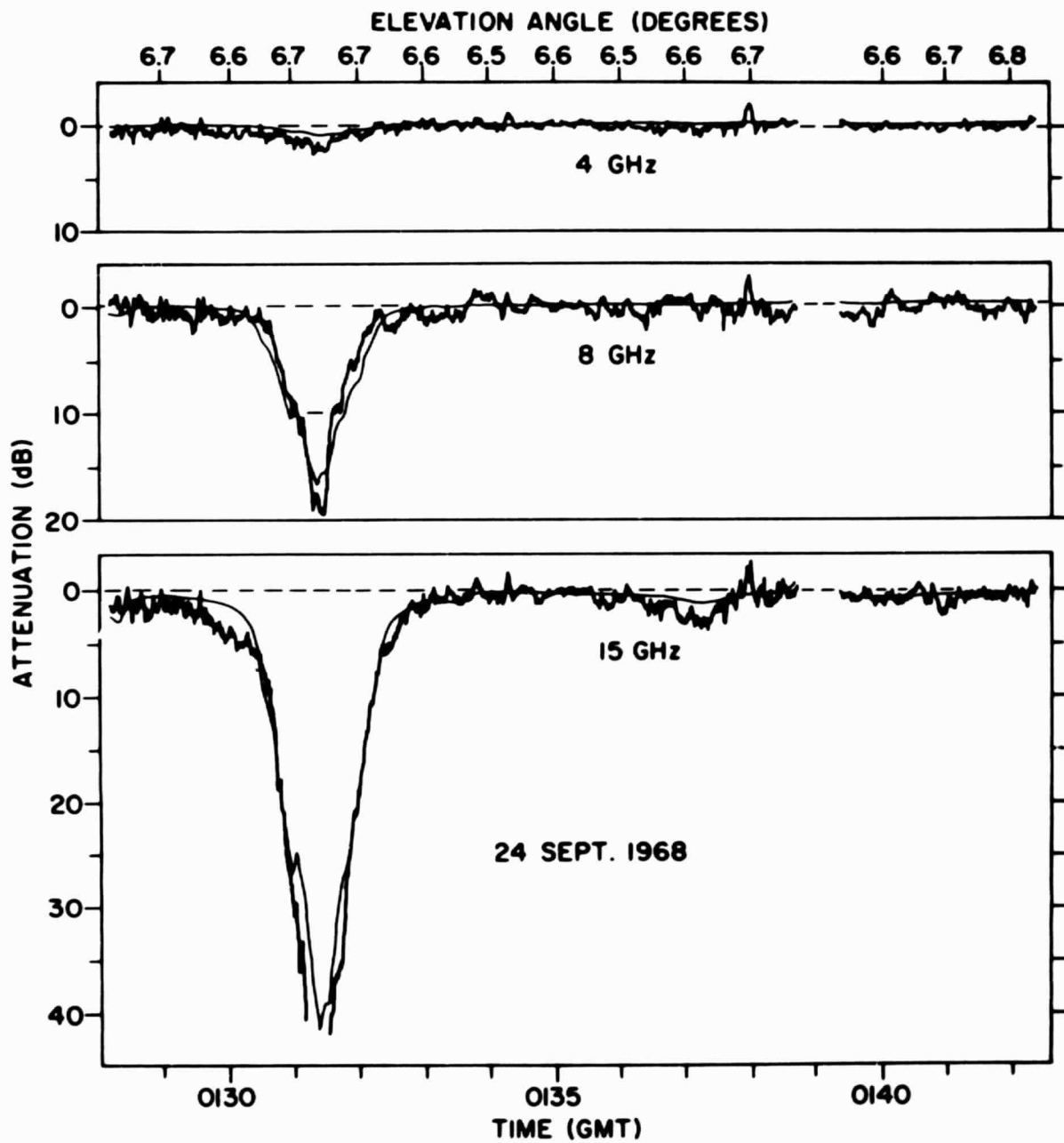
Fig. 12:   Comparisons of attenuations measured by ATS-6 satellite
            receivers at 13 and 18 GHz (heavy curves) with that predicted
            by radar data combined with raingage and disdrometer data for
            a storm in Virginia during 1975. [from Goldhirsh (1976)].

Figure axis labels: Fade Depth (dB) — vertical axis; Time, GMT (hr: min) — horizontal axis.

18 GHz (Measured)

13 (GHz (Measured)

18 GHz (Predicted)

13 GHz (Predicted)
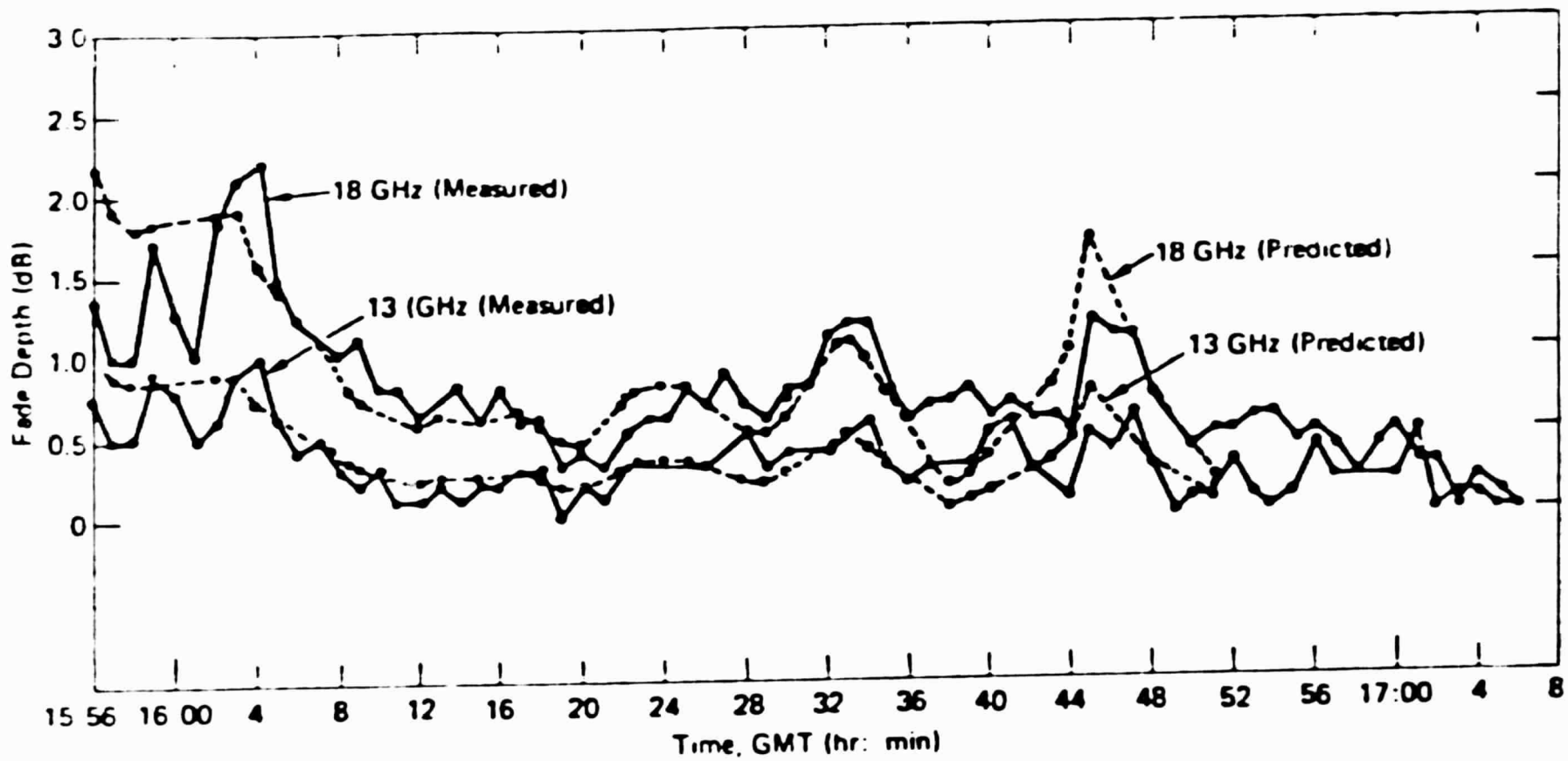
Fig. 13:   Attenuation A versus reflectivity factor Z_e for a storm in
           Sudbury, Massachusetts, during 1971. The open circles, solid
           circles and crosses represent experimental points measured by
           a dual-wavelength radar with wavelengths of 0.86 and 5.6 cm at
           three different altitudes in the storm. The straight line is
           an empirical fit to A-Z data computed from disdrometer data
           at the ground. The curve at the top illustrates the relative
           number of radar profiles used in computing the experimental
           data points [from Joss et al. (1974)].

27 Aug 1971 1001-1200 EST
Sudbury, Mass.

$Z = 1360\, A^{1.38}$

DSD at ground
○ Radar 580 - 1860 m
× " 1860 - 3140 m
● " 3140 - 4420 m
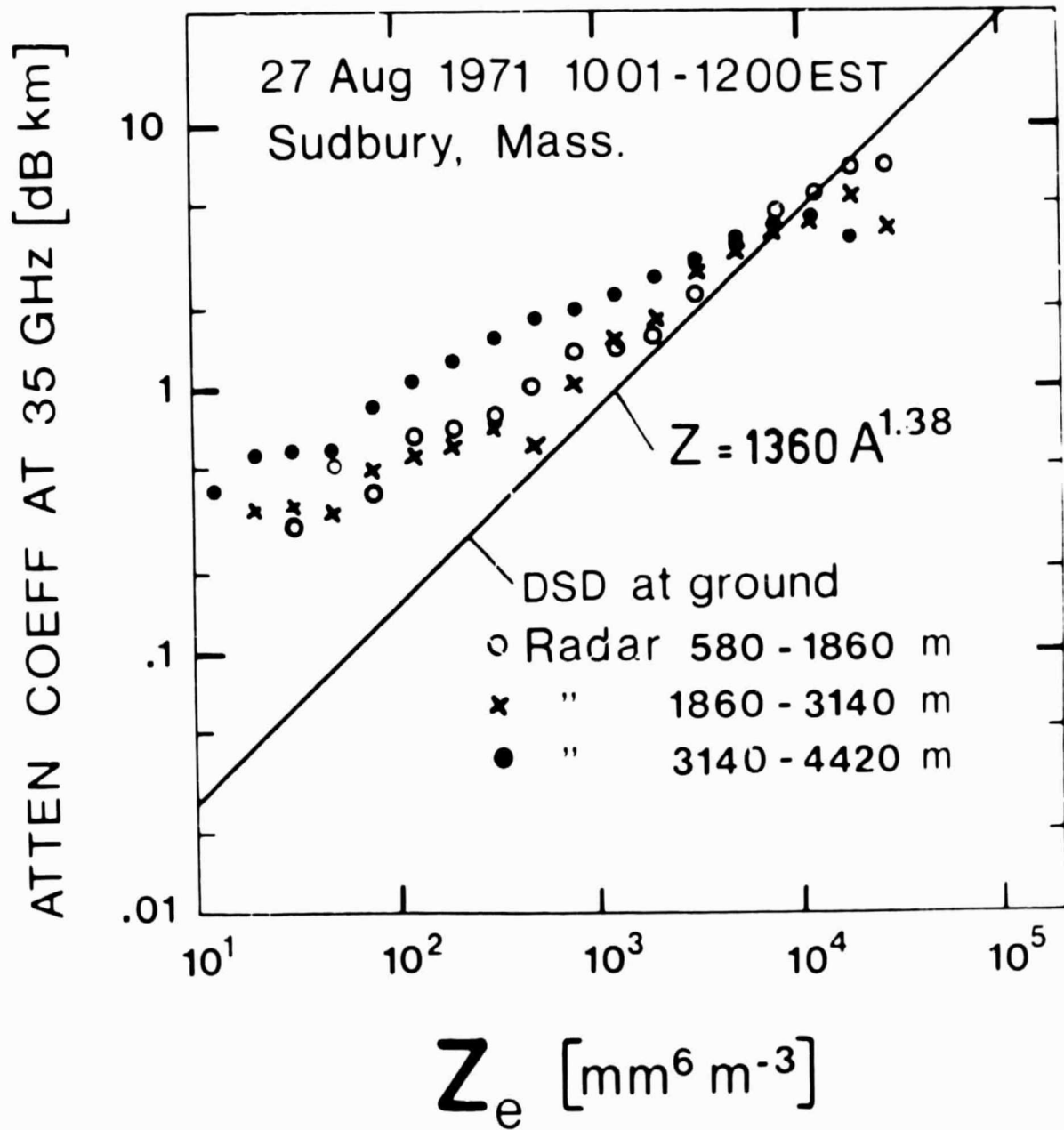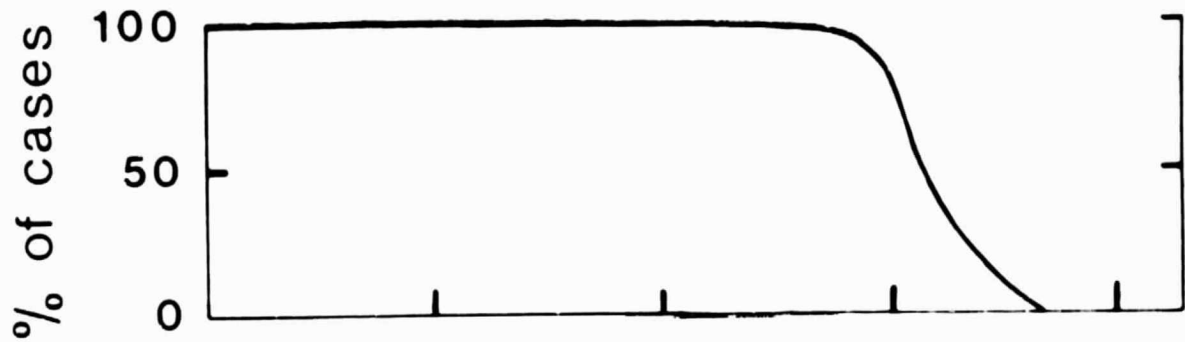
Fig. 14: Cross correlation functions between the logarithm of
          reflectivity factor measured aloft at several altitudes by
          radar and the logarithm of reflectivity factor calculated
          from disdrometer data at the surface versus time lag τ. The
          radar and disdrometer are the same as those in Fig. 13.
          [from Joss et al. (1974)].

27 Aug 1971 1001-1226 Sudbury, Mass.
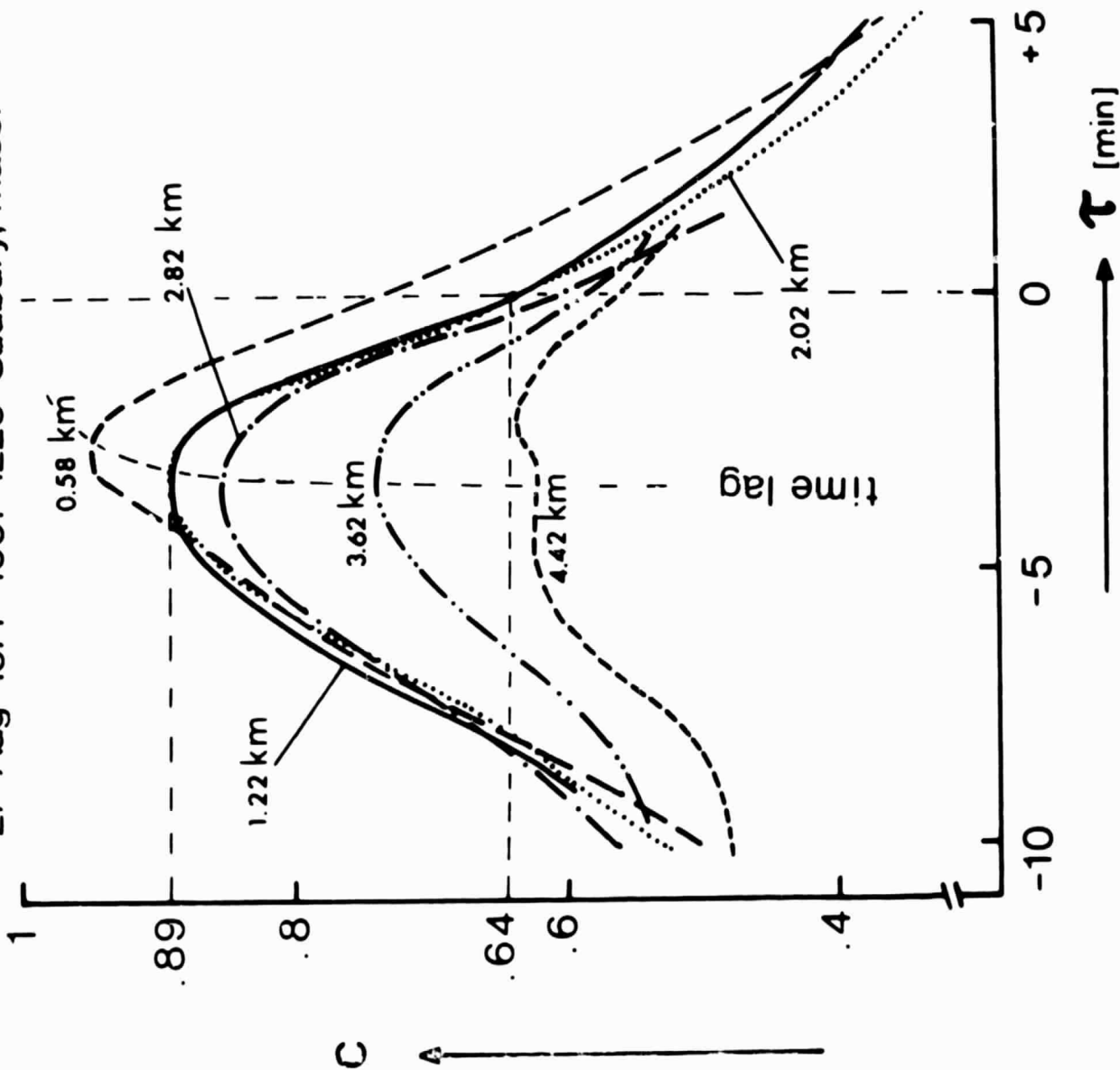
Fig. 15:   Average reflectivity factor Z measured below the bright band
            by an X-band radar versus rainfall rate deduced from
            attenuation measured by a K_a-band radar. Both nadir-pointing
            radars were colocated on an aircraft flying over the ocean.
   [from Masuko et al. (1981)].

JUNE 15, 1981
15:53–16:09

$Z = 126.34R^{1.59}$

RADAR REFLECTIVITY FACTOR Z(X-BAND)

RAINFALL RATE(mm/h) DERIVED FROM
Ka BAND ATTENUATION
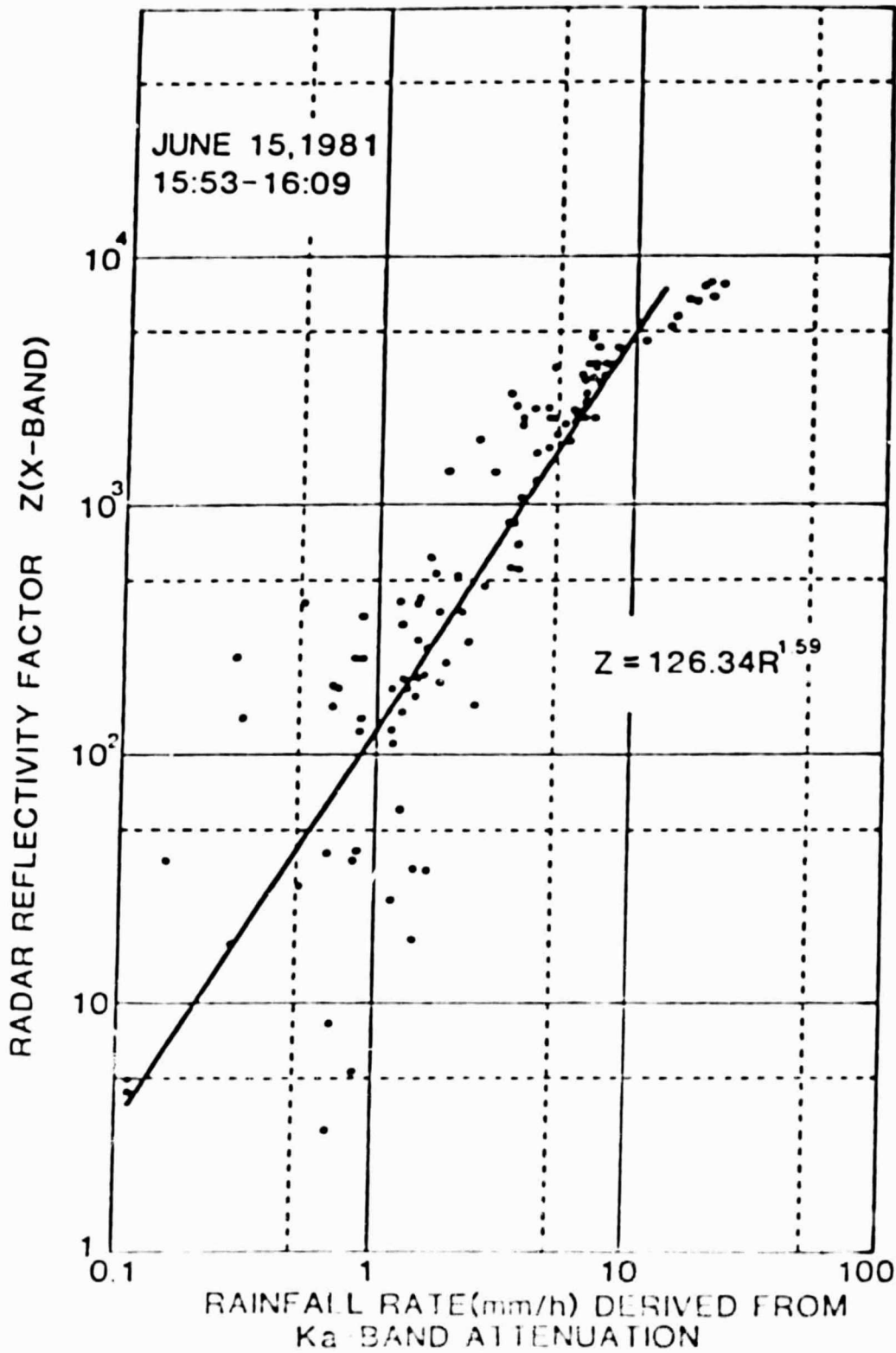
Fig. 16:   Microwave brightness temperature at X-band (left figure) and
at K_a-band (right figure) versus rainfall rate deduced from
attenuation of the K_a-band radar in Fig. 15.   The solid circles
are measured data points.   The solid curves represent least
squares fits of second degree polynomials to the data points.
[from Masuko et al. (1981)].

October 20, 1980
Bright Band Height : 3680 m
r = 0.91

$T = -1.14E - 01 \cdot R^2 + 5.42 \cdot R + 126.84$

$\overline{T_0^{SEA}} = 126.8$ K

October 20, 1980
Bright Band Height : 3680 m

$T_0^{SEA} = 177.3$ K
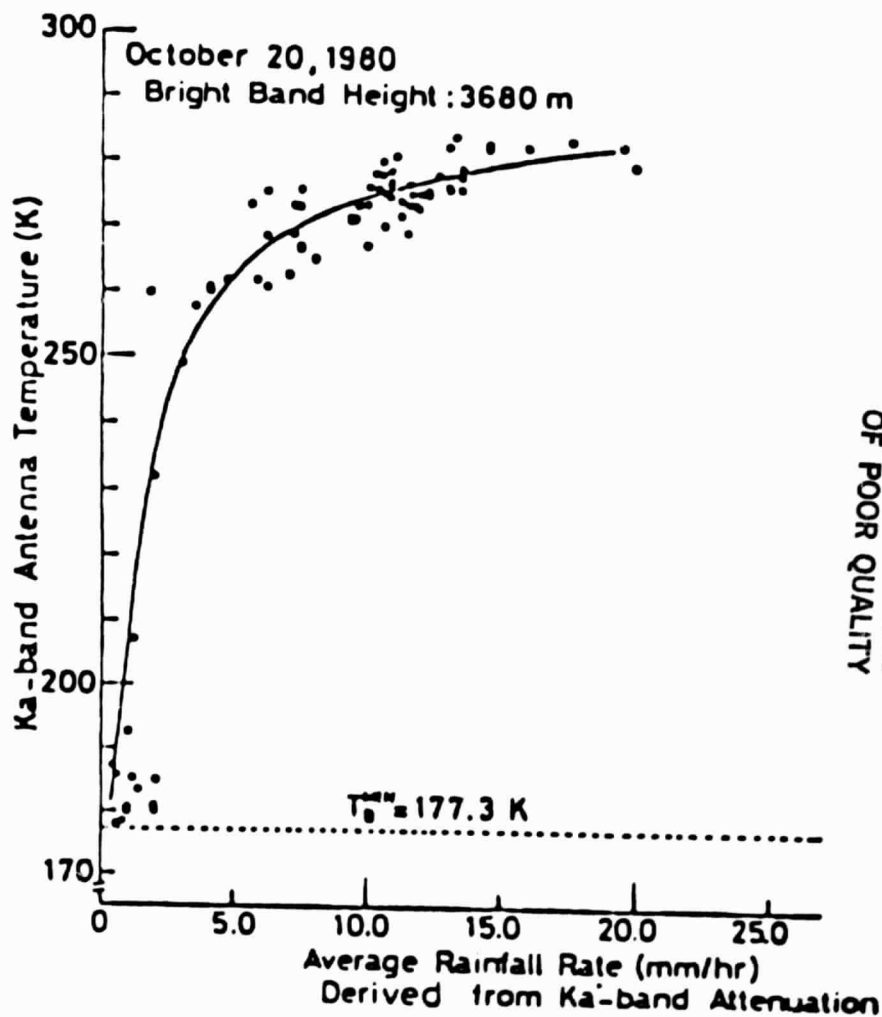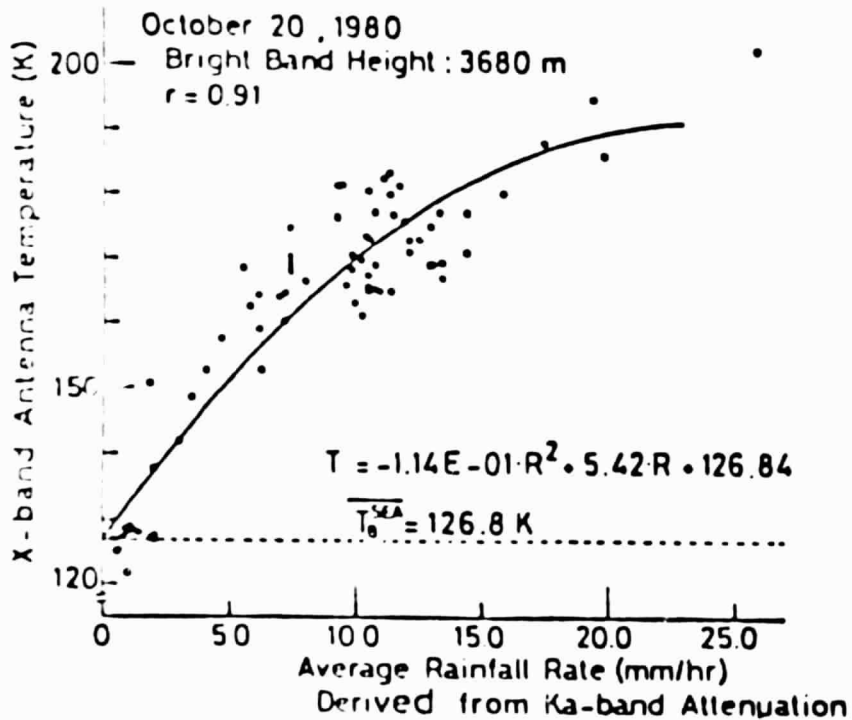
Fig. 17:   Theoretical curves of differential reflectivity factor Z_{DR}(db) and reflectivity factor at horizontal polarization Z_H ($m^{-3}cm^{-1}$) divided by N_0($m^{-3}cm^{-1}$) versus median volume diameter D_0 for an exponential drop size distribution with maximum drop diameter D_{max} = 0.8 cm. [from Seliga et al. (1981)]
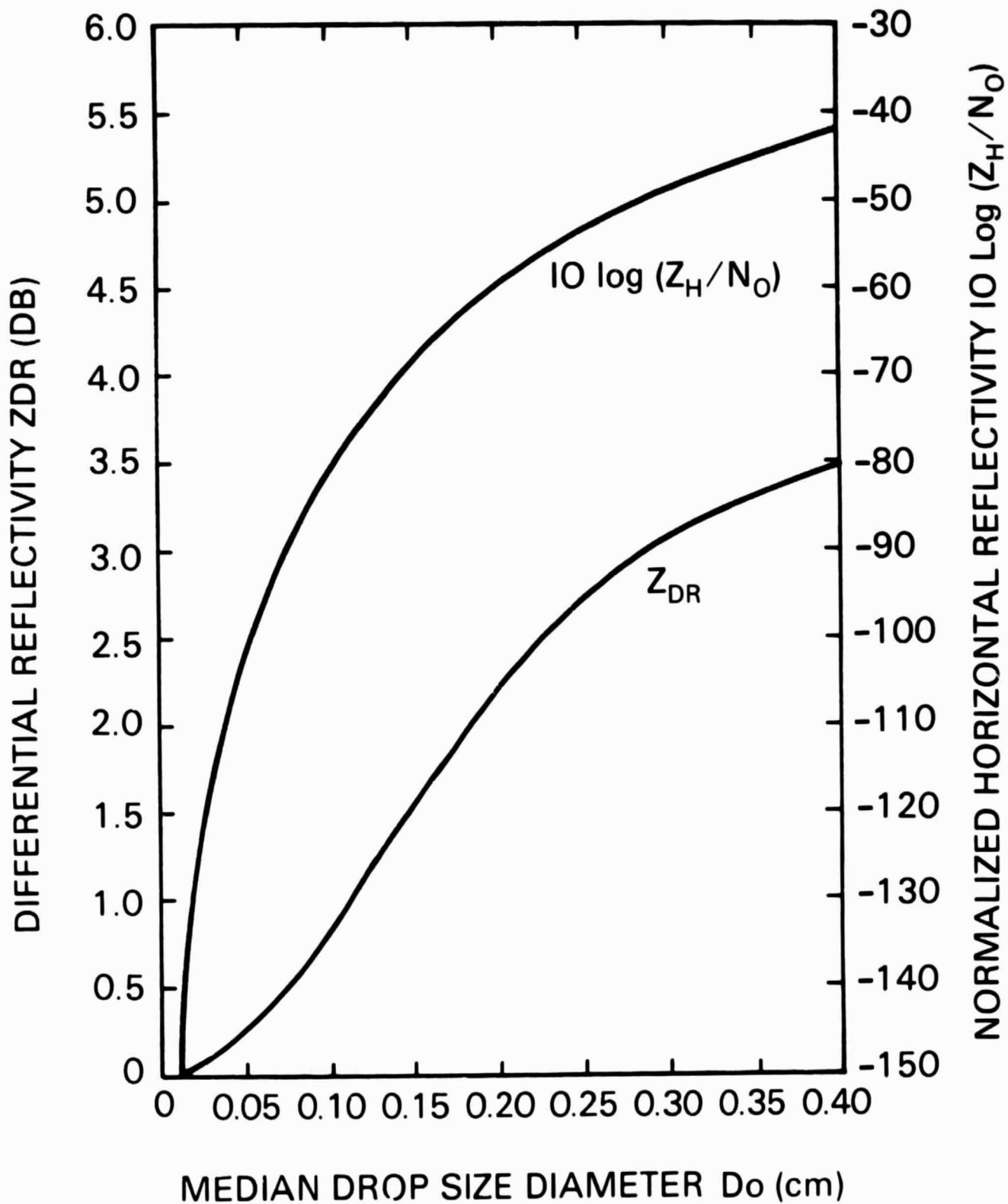
Fig. 18:   Left: Comparison of total path attenuation A_R deduced from dual-
polarization data with A_D, that measured directly from an
11.6 GHz beacon on the ESA geostationary OTS. The solid circles
and crosses are measured data points, the latter corresponding
to cases where the melting layer contribute at least half the
total attenuation. The measurements were made in two storms
during October 1979 in Southern England.

Right: Comparison of raingage-derived total path attenuation, $\bar{A}^r$
with that measured directly $\bar{A}_D$. All data were averaged over
time intervals of 4 minutes. Other details the same as
at left. [from Hall et al. (1980c)].
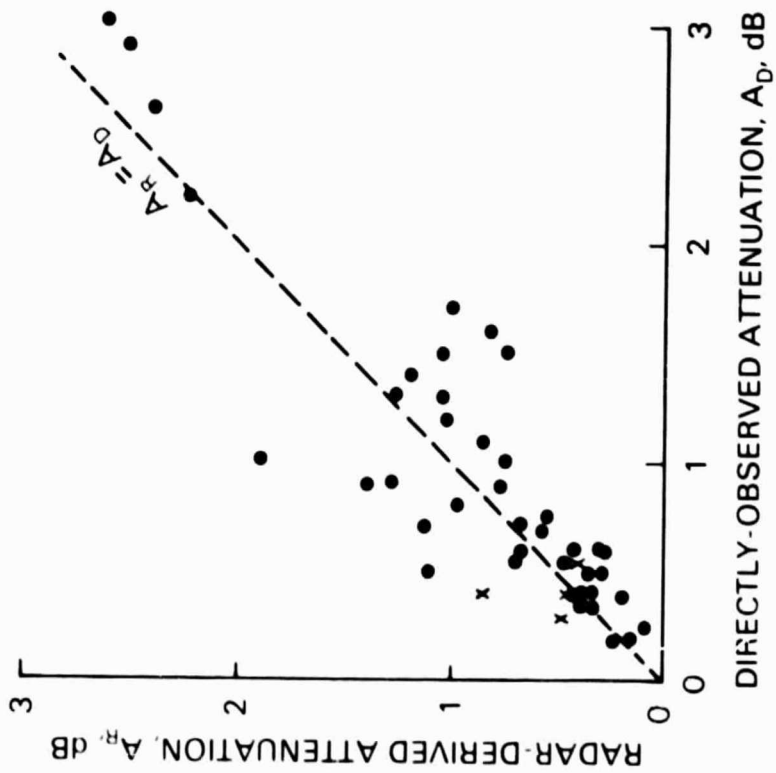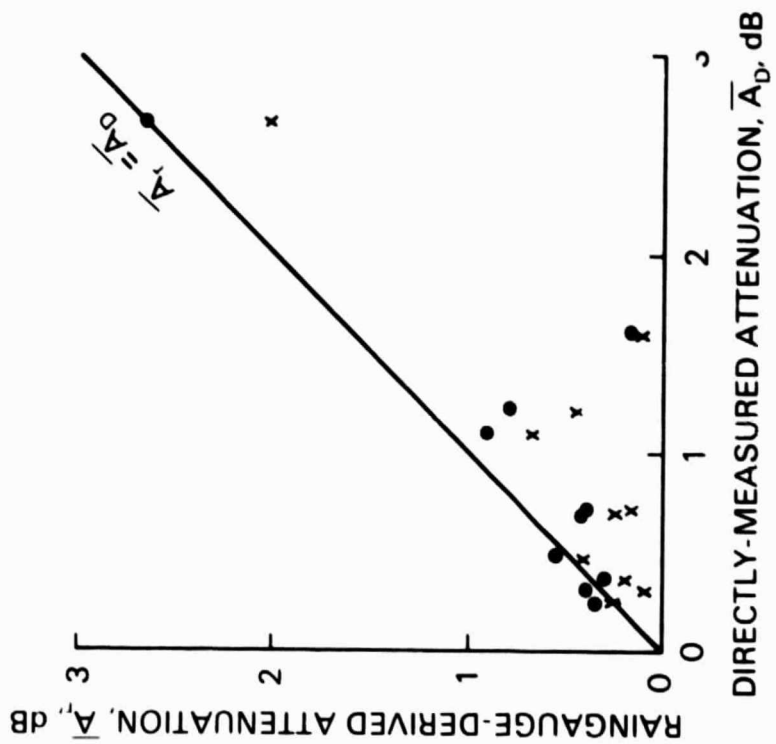
Fig. 19:   Time sequence of (a) Z_{DR} and (b) Z_H as determined from radar
and disdrometer data. Solid curves calculated from 30s
averages of disdrometer data using backscattering cross
sections at horizontal and vertical polarizations as described
by Seliga and Bringi (1979). Solid circles are radar-measured
30s averages with the antenna fixed. Open circles are radar-
measured data with the antenna scanning at $1^{o} s^{-1}$. The dashed
curve is the recalculated Z_{DR} using the modified backscattering
cross sections of Goddard et al. (1982). [from Goddard et al.
(1982)].